Research Papers

Resiliency assessment of the distribution system considering smart homes equipped with electrical energy storage, distributed generation and plug-in hybrid electric vehicles

Pourya Jafarpour [a], Mehrdad Setayesh Nazar [a], Miadreza Shafie-khah [b], João P.S. Catalão [c,*]

[a] *Shahid Beheshti University (SBU), Tehran, Iran*
[b] *Univ. Vaasa, 65200 Vaasa, Finland*
[c] *Faculty of Engineering of the University of Porto (FEUP) and INESC TEC, 4200-465 Porto, Portugal*

A B S T R A C T

This paper presents a novel method for resiliency assessment of the distribution system considering smart homes' arbitrage strategies in the day-ahead and real-time markets. The main contribution of this paper is that the impacts of smart homes' arbitrage strategy on the resilient operation of the distribution system are explored. The optimal commitment of smart homes in external shock conditions is another contribution of this paper. An arbitrage index is proposed to explore the impacts of this process on the system costs and resiliency of the system. A two-level optimization process is proposed for day-ahead and real-time markets. At the first stage of the first level, the optimal bidding strategies of smart homes are estimated for the day-ahead market. Then, the database is updated and the optimal bidding strategies of smart homes for real-time horizon are assessed in the second stage of the first level problem. At the first stage of the second level problem, the optimal day-ahead scheduling of the distribution system is performed considering the arbitrage and resiliency indices. At the second stage of the second level, the distribution system optimal scheduling is carried out for the real-time horizon. Finally, at the third stage of the second level, if an external shock is detected, the optimization process determines the optimal dispatch of system resources. The proposed method is assessed for the 33-bus and 123-bus IEEE test systems. The proposed framework reduced the expected values of aggregated costs of 33-bus and 123-bus systems by about 62.14 % and 32.06 % for the real-time horizon concerning the cases in which the smart homes performed arbitrage strategies. Furthermore, the average values of the locational marginal price of 33-bus and 123-bus systems were reduced by about 59.38 % and 63.98 % concerning the case that the proposed method was not implemented.

1. Introduction

The optimal resilient operation of distribution systems considering the smart home contribution scenarios is an important issue in operational paradigms of electrical systems. The smart homes concept is widely utilized in recent papers to increase the efficiency of energy conversion, resiliency, and flexibility of electrical systems. Smart home commitment in the external shock condition is an optimization process that depends on the hierarchical architecture of control systems, smart homes' locations, load density, communication infrastructure design, consumers' comfort levels, and other technical and economic parameters of the electrical system. The Distribution System Operator (DSO) can improve the resiliency of its system using the optimal commitment of

smart homes and other distributed energy resources to reduce the impacts of external shocks [1]. A smart home can be equipped with Electrical Storage Systems (ESSs), Plug-in Hybrid Electric Vehicles (PHEVs), fossil-fueled Distributed Generation (DG) facilities, Intermittent Power Generation (IPG) facilities, and smart appliances. Further, smart homes can participate in distribution system Demand Response Programs (DRPs) [2]. The distribution system operator should coordinate its system resources considering the smart homes arbitrage opportunities in the operational scheduling horizons.

Over recent years, different aspects of resilient operational scheduling of distribution systems are presented considering the optimal commitment of Distributed Energy Resources (DERs) and switching of system switches. As shown in Table 1, the literature can be categorized into the following categories. The first category considers the aspects of

Nomenclature

Abbreviation

ARIMA	Autoregressive Integrated Moving Average
CMSH	Comfort Mode of Smart Home
SMSH	Saver Mode of Smart Home
EPSH	Energy Partner Mode of Smart Home
DA	Day-Ahead
DER	Distributed Energy Resource
DG	Distributed Generation
DRP	Demand Response Program
DSO	Distribution System Operator
ESS	Electrical Energy Storage
IPG	Intermittent Power Generation
MILP	Mixed Integer Linear Programming
MINLP	Mix Integer Non-Linear Programming
MT	Micro Turbine
MU	Monetary Unit
PHEV	Plug-in Hybrid Electrical Vehicle
PV	PhotoVoltaic
RT	Real-Time
RTLF	Real-Time Load Forecasting
WT	Wind Turbine

Sets

NSHOS	Set of operational states of smart homes
NSL	Set of shed loads
NCS	Set of contingent conditions
NB	Set of buses
NST	Set of system topology
NDSRT	Set of distribution system real-time contingent conditions

Parameters

ξ^{SR}	Price of spinning reserve in day-ahead market (MUs/kW)
ξ^{active}	Price of active power in day-ahead market (MUs/kWh)
$\xi^{reactive}$	Price of reactive power in day-ahead market (MUs/kVARh)
$Prob$	Probability of scenario
W	Weighting factor
CIC	Customer interruption costs (MUs)

Variables

$C_{SH}^{X\ DA}$	Smart home distributed energy resources day-ahead costs $\forall X \in$ IPG, DG, ESS, PHEV(MUs)
$C_{SH}^{Purchase\ DA}$	Smart home day-ahead energy purchased costs (MUs)
$B_{SH}^{Sell\ DA}$	Smart home day-ahead energy sold benefits (MUs)
$B_{SH}^{DRP\ DA}$	Smart home day-ahead demand response program contribution benefits (MUs)
$B_{SH}^{AR\ DA}$	Smart home day-ahead arbitrage benefits (MUs)
$Penalty^{active\ DA}$	Penalty of arbitrage of smart homes in day-ahead active power market (MUs)
$Penalty^{reactive\ DA}$	Penalty of arbitrage of smart homes in day-ahead reactive power market (MUs)
SR_{DA}^{SH}	Spinning reserve provided by smart home for day-ahead market (kW)
P_{DA}^{SH}	Active power provided by smart home for day-ahead market (kW)
Q_{DA}^{SH}	Reactive power provided by smart home for day-ahead market (kVAR)
P_{SH}^{X}	Smart home distributed energy resources active power $\forall X \in$ IPG, DG, ESS, DRP, PHEV(kW)
P_{SH}^{Load}	Smart home active power of load (kW)
P_{SH}^{Loss}	Smart home active power loss (kW)
Q_{SH}^{X}	Smart home distributed energy resources reactive power $\forall X \in$ DG, DRP, PHEV(kVAR)
Q_{SH}^{Load}	Smart home reactive power of load (kVAR)
Q_{SH}^{Loss}	Smart home reactive power loss (kVAR)
$P_{SH\ Dispatchable}^{Load}$	Smart home dispatchable active power (kW)
$P_{SH\ Deferrable}^{Load}$	Smart home deferrable active power (kW)
$P_{SH\ Non-dispatchable}^{Load}$	Smart home non-dispatchable active power (kW)
ΔP_{SH}^{TOU}	Active power change of smart home based on time-of use program (kW)
ΔP_{SH}^{DLC}	Active power change of smart home based on direct load control program (kW)
$C_{SH}^{X\ RT}$	Smart home distributed energy resources real-time costs $\forall X \in$ IPG, DG, ESS, PHEV(MUs)
$C_{SH}^{Purchase\ RT}$	Smart home real-time energy purchased costs (MUs)
$B_{SH}^{Sell\ RT}$	Smart home real-time energy sold benefits (MUs)
$B_{SH}^{DRP\ RT}$	Smart home real-time demand response program contribution benefits (MUs)
$B_{SH}^{AR\ RT}$	Smart home real-time arbitrage benefits (MUs)
$Penalty^{active\ RT}$	Penalty of arbitrage of smart homes in real-time active power market (MUs)
$Penalty^{reactive\ RT}$	Penalty of arbitrage of smart homes in real-time reactive power market (MUs)
P_{RT}^{SH}	Active power provided by smart home for real-time market (kW)
Q_{RT}^{SH}	Reactive power provided by smart home for real-time market (kVAR)
$C_{DS}^{X\ DA}$	Distribution system distributed energy resources day-ahead costs $\forall X \in$ IPG, DG, ESS, PLOT(MUs)
$C_{DS}^{Purchase\ DA}$	Distribution system day-ahead energy purchased from upward network costs (MUs)
$B_{DS}^{Sell\ DA}$	Distribution system day-ahead energy sold to consumers benefits (MUs)
$C_{DS}^{DRP\ DA}$	Distribution system day-ahead demand response program contribution costs (MUs)
$C_{DS}^{AR\ DA}$	Distribution system day-ahead arbitrage cost (MUs)
$ENSC$	Energy not supplied costs (MUs)
RI	Resiliency index
ARI	Arbitrage index
LMP	Locational marginal price (MUs)
P_{DS}^{X}	Distribution system distributed energy resources active power $\forall X \in$ IPG, DG, ESS, PLOT (kW)
P_{Custom}^{Load}	Distribution system active power of custom load (kW)
P_{DS}^{Loss}	Distribution system active power loss (kW)
P_{DS}^{IMPORT}	Distribution system imported active power from upward network (kW)
$C_{DS}^{X\ RT}$	Distribution system distributed energy resources real-time costs $\forall X \in$ IPG, DG, ESS, PLOT(MUs)
$C_{DS}^{Purchase\ RT}$	Distribution system real-time energy purchased from upward network costs (MUs)
$B_{DS}^{Sell\ RT}$	Distribution system real-time energy sold to consumers benefits (MUs)
$C_{DS}^{DRP\ RT}$	Distribution system real-time demand response program contribution costs (MUs)
$C_{DS}^{AR\ RT}$	Distribution system real-time arbitrage cost (MUs)
y	Binary decision variable of boundary line

Table 1
Comparison of the proposed method with other papers.

References	3	4	5	6	7	8	9	10	11	12	13	14	15	16	17	18	19	20	21	22	23	24	25	26	27	28	29	30	31	32	33	34	35	36	37	38	39	40	Proposed Approach
Arbitrage of smart homes	×	×	×	×	×	×	×	×	×	×	×	×	×	×	×	×	×	×	×	×	×	×	×	×	×	×	×	×	×	×	×	×	×	×	×	×	×	×	✓
Switching of system in ext. shock	×	×	✓	×	×	×	✓	×	×	×	✓	×	×	×	×	×	×	×	×	×	×	×	×	×	✓	✓	✓	✓	✓	✓	×	✓	×	×	×	×	×	×	✓
Categorization of smart homes modes	×	×	×	×	×	×	×	×	×	×	×	×	×	×	×	×	×	×	×	×	×	×	×	×	×	×	×	×	×	×	×	×	×	×	×	×	×	×	✓
Modeling of LMP considering smart homes commitment	×	×	×	×	×	×	×	×	×	×	×	×	×	×	×	×	×	×	×	×	×	×	×	×	×	×	×	×	×	×	×	×	×	×	×	×	×	×	✓
Real-time pricing	×	×	×	×	×	×	×	×	×	✓	×	×	×	×	✓	×	×	×	✓	×	×	×	×	×	✓	×	×	×	×	×	×	×	×	×	×	×	×	×	✓
DLC	×	×	✓	×	×	✓	×	×	✓	×	×	✓	×	×	✓	×	×	✓	×	×	✓	✓	✓	×	×	✓	×	×	×	×	×	×	×	×	×	×	×	×	✓
Ancillary service of smart homes	×	×	×	×	×	✓	×	✓	✓	×	×	×	×	×	×	×	×	×	×	×	×	×	×	×	×	×	×	×	×	×	×	×	×	×	×	×	×	×	✓
Resiliency index	×	×	✓	×	×	×	✓	×	×	×	×	×	×	×	×	×	×	×	×	×	×	×	×	×	×	×	×	×	×	×	×	✓	×	×	✓	×	×	×	✓
Arbitrage index	×	×	×	×	×	×	×	×	×	×	×	×	×	×	×	×	×	×	×	×	×	×	×	×	×	×	×	×	×	×	×	×	×	×	×	×	×	×	✓
Method MILP	✓	✓	✓	×	✓	×	×	×	×	×	✓	×	×	×	✓	×	×	×	×	✓	×	✓	✓	×	✓	×	×	×	✓	×	×	×	×	×	×	×	×	×	×
MINLP	×	×	×	×	×	×	×	×	×	×	×	✓	✓	×	×	×	×	×	×	×	×	×	×	×	×	×	×	✓	×	×	×	✓	×	×	×	×	×	×	×
Heuristic	×	×	×	×	×	×	×	×	×	×	×	×	×	✓	×	✓	✓	✓	✓	×	×	×	✓	×	×	✓	✓	✓	×	✓	✓	×	✓	✓	×	✓	✓	✓	✓
Model Determ.	×	✓	×	×	×	×	✓	✓	×	×	✓	✓	×	✓	×	✓	✓	✓	✓	×	×	×	×	×	✓	×	×	×	✓	✓	✓	✓	×	✓	×	×	×	×	×
Stoch.	✓	×	✓	×	×	×	×	×	✓	×	×	✓	×	✓	×	×	×	×	×	✓	✓	×	✓	✓	×	×	✓	×	×	×	×	×	×	×	✓	✓	✓	✓	✓
Objective Function Revenue	×	×	×	×	×	×	×	×	×	×	×	×	×	×	×	×	×	×	×	×	×	✓	✓	✓	×	×	×	✓	×	×	×	×	✓	×	×	×	×	×	✓
Gen. Cost	✓	✓	✓	×	✓	×	×	×	×	×	✓	✓	✓	×	✓	×	×	✓	✓	✓	×	✓	✓	✓	✓	✓	✓	✓	✓	✓	✓	✓	×	✓	✓	✓	✓	✓	✓
Storage Cost	✓	✓	✓	×	✓	×	×	×	×	×	×	✓	✓	✓	✓	×	×	✓	✓	✓	×	✓	✓	✓	×	×	✓	×	×	×	×	×	×	✓	×	×	×	×	✓
Secu. Costs	×	×	×	×	×	×	✓	×	×	×	×	✓	×	×	×	×	✓	×	×	✓	✓	×	✓	×	✓	✓	×	×	×	✓	✓	✓	✓	✓	✓	✓	✓	✓	✓
PHEV cost	×	×	×	×	×	×	×	×	×	×	✓	×	×	✓	✓	✓	×	✓	×	×	✓	×	✓	×	×	×	×	×	×	×	×	✓	×	×	×	×	×	×	✓
DRP costs	×	×	×	×	✓	×	×	✓	×	×	✓	✓	×	✓	✓	×	×	✓	✓	×	✓	✓	×	✓	✓	×	×	×	×	×	×	✓	×	×	×	×	×	×	✓
WT	✓	×	×	×	×	×	×	×	×	×	×	✓	×	×	✓	×	✓	×	✓	×	×	✓	×	×	×	×	×	×	✓	×	×	✓	×	✓	×	✓	×	×	✓
PV	✓	✓	✓	×	×	×	×	×	×	×	×	✓	×	✓	✓	×	✓	×	✓	✓	×	✓	×	×	×	×	×	×	×	×	×	×	×	×	×	×	×	×	✓
DA-Market	✓	✓	✓	×	✓	×	×	×	×	×	✓	×	✓	×	✓	✓	✓	✓	×	✓	×	✓	✓	✓	✓	✓	✓	✓	✓	×	✓	×	×	✓	×	✓	✓	✓	✓
RT- Market scheduling	×	×	×	×	×	×	×	×	×	×	×	×	×	×	✓	×	×	×	×	✓	×	×	×	×	×	×	×	×	×	×	×	×	×	✓	×	×	×	×	✓
Uncertainty Model PHEV	×	×	×	×	×	×	×	×	×	×	×	×	×	✓	×	✓	×	×	×	×	✓	×	✓	×	✓	×	×	×	×	×	×	✓	×	×	×	×	×	×	✓
DRP	×	×	×	×	×	×	×	×	×	✓	×	×	×	×	×	×	×	×	×	×	✓	✓	×	✓	×	×	×	×	×	×	×	✓	×	×	×	×	×	×	✓
DA Market price	×	×	×	×	×	×	×	×	×	×	×	×	×	×	×	×	×	×	×	×	×	✓	×	×	×	×	×	×	×	×	×	✓	×	×	×	×	×	×	✓
RT Market price	×	×	×	×	×	×	×	×	×	×	×	×	×	×	×	×	×	×	×	×	×	✓	×	×	×	×	×	×	×	×	×	✓	×	×	×	×	×	×	✓
External Shock	×	×	×	×	×	×	✓	×	×	×	✓	×	×	×	×	×	×	×	×	×	×	✓	×	×	×	×	×	×	×	×	×	×	×	×	×	✓	✓	✓	✓
Loads	×	×	×	×	×	×	×	×	✓	✓	×	×	×	×	×	×	×	×	×	×	×	×	✓	×	×	×	×	×	×	×	×	×	×	×	×	×	×	×	✓
Inter. electricity generation	✓	×	×	×	×	×	×	×	×	×	×	×	✓	×	✓	×	×	×	✓	×	×		×	×	×	×	×	×	✓	×	×	×	×	×	×	✓	×	×	✓

smart home commitment in distribution system operational scheduling [3–27]. The optimal resilient scheduling of the distribution system considering smart homes contributions can be categorized into the following subgroups: 1) load commitment strategies [3–16], 2) PHEVs commitment strategies [17–21], and 3) combinations of the above strategies [22–27].

Based on the above categorization and for the first subgroup, Ref. [3] introduced a tri-level optimization algorithm to maintain the resiliency of the system in external shock conditions. The first level optimized the

system's energy transactions, the second level determined the transacted energy between utility and smart homes, and the third level optimized the energy costs of smart homes. Ref. [4] assessed the resiliency of buildings equipped with energy storage and photovoltaic arrays. The results showed that the resiliency of buildings was highly improved using the photovoltaic and energy storage facilities. Ref. [5] evaluated a robust optimization process to enhance the resiliency of the system using demand response programs. The proposed method considered the uncertainties of external shocks, intermittent power generations, and load

and price parameters. Ref. [6] proposed an event-based demand response program to improve the system resiliency and considered the behavior of residential consumers using the game theory model. Ref. [7] introduced a two-level optimization process for load commitment of smart homes. The first level minimized the smart homes' energy costs, and the second level minimized the deviations of load profiles. Ref. [8] assessed a distributed real-time demand response process to carry out the load curtailment process and increase the flexibility and resiliency of the system. Ref. [9] introduced the load curtailment process using the Markov model and multiple resiliency indices to assess the resiliency of the system. The Monte Carlo simulation procedure was utilized to evaluate the proposed indices. Ref. [10] proposed an optimization algorithm for procuring regulation reserve services considering demand response alternatives. The optimization algorithm utilized a dynamic programming method to optimize the system costs considering the system's contingencies. Ref. [11] assessed a load control process to determine the maximum admissible time for disconnecting the loads. The results showed that for the UK power system about 200 MW of 22 GW could be controlled in critical conditions. Ref. [12] introduced a real-time pricing algorithm to minimize the peak-to-average demand ratio. The proposed algorithm maximized the social welfare and optimized the consumers' power consumption. Ref. [13] evaluated an optimization process to minimize load curtailments of the system in the contingent condition considering uncertainties. The optimal scheduling of system resources was determined by a robust optimization algorithm. Ref. [14] introduced a resilient optimization model to supply the critical loads in external shock conditions that committed adjustable loads. The load shedding was minimized and the served non-critical loads were maximized. Refs. [3–14] did not consider smart homes' commitment modes, arbitrage opportunities, resiliency index, and locational marginal price in their proposed models.

Other papers modeled the load commitment procedures for smart homes without considering the system's resiliency. Ref. [15] presented a day-ahead scheduling load commitment process using a reinforcement algorithm. The agent-based optimization algorithm found the optimal sequence of load commitment for the scheduling interval. Renewable power generation was considered in the proposed model. However, the resiliency of the system was not modeled. Ref. [16] proposed a two-stage optimization algorithm for optimal demand response coordination of residential space heating loads. The model considered day-ahead and balancing markets. The first stage model minimized the customers' payments and the second stage problem maximized the customers' bonus. However, the resiliency of the system and the arbitrage opportunities were not modeled in Refs. [15,16].

Based on the above categorization and for the second subgroup, Ref. [17] introduced a two-stage stochastic optimization framework for optimal scheduling of microgrids considering PHEVs' contributions to improving the resiliency of the system. Ref. [18] assessed an algorithm that committed PHEVs in external shock conditions to improve the resiliency of the distribution system. The optimization algorithm minimized the maximum electrical power of turned-on smart appliances that were supplied by PHEVs. Ref. [19] analyzed the reliability of the system considering vehicle-to-grid and vehicle-to-home modes of operations. The results showed that the reliability of the system was increased using the vehicle to grid process in the external shock conditions. Ref. [17–19] did not consider smart home arbitrage opportunities, optimal resilient switching of the distribution system, and locational marginal price in their proposed models.

Other papers modeled the PHEVs commitment process for smart homes without considering the resiliency of the system. Ref. [20] assessed an optimization model that simultaneously optimized the objective function of the system operator, distribution generation owner, intermittent electricity generations, and parking lot of PHEVs. The simulation was carried out for the 33-bus IEEE test system. Ref. [21] presented an algorithm for optimizing PHEV commitment considering the time-of-use demand response tariff. The model compromised

photovoltaic arrays and electrical energy storage systems and the optimization process minimized customers' costs. The resiliency of the system was not modeled in Refs. [20,21].

For the third category of subgroup, Ref. [22] introduced an algorithm for the optimal commitment of loads and PHEVs. The optimization process minimized the system costs and inconvenience of customers. Ref. [23] assessed an online optimization process to increase the resiliency of islanded microgrid using PHEVs and electrical energy storage. Ref. [24] presented an optimization framework to increase the resiliency of the system considering intermittent electricity generations, energy hubs, demand response programs, and PHEVs. Ref. [25] evaluated a two-stage optimization process for building microgrids for day-ahead and real-time optimization intervals. The building was equipped with energy storage, PHEVs, and intermittent electricity generation. The proposed algorithm increased the resiliency of buildings considering the customers' comfort level. Ref. [26] assessed an optimization process that considered aging and reliability as objective functions. The model utilized emergency demand response as an energy resource to increase the resiliency of the system. The results showed that the demand response reduced the aging of system facilities and system costs. Ref. [27], introduced a stochastic optimization algorithm to increase the resiliency of the system considering demand response programs and PHEVs. The optimization process utilized a conditional value at risk model to find the best risk-averse values of system costs. Refs. [22–27] did not consider smart homes contribution modes, arbitrage opportunities, optimal resilient switching of the distribution system, and locational marginal price in their proposed models.

The second category of papers optimized the operational scheduling of the system in external shock conditions utilizing the concept of a self-healing process and switching of normally opened/closed switches to improve the resiliency of the system [28–36]. These papers investigated the optimal switching of the distribution system for pre-event and/or post-event conditions. Ref. [28] investigated a sectionalizing process to increase the resiliency of the distribution system and schedule the distributed energy resources. An optimization algorithm was performed that utilized the stochastic model of the system to minimize the operational costs system and restore the system after tolerating an external shock. Ref. [29] assessed an optimization algorithm for the resilient scheduling of the distribution system using graph theory. The model utilized the Tabu search algorithm to minimize disconnected loads, energy losses, and load-generation imbalance. Ref. [30] analyzed a two-stage algorithm that simultaneously scheduled microgrids and distribution systems. In the first stage, the commitment schedule of microgrids was optimized and in the second stage, the distribution system was restored using the capacity of microgrids to reduce the unserved energy. The centralized and hierarchical optimization algorithms for scheduling were considered and the centralized approach had better results concerning another method. Ref. [31] introduced resilient scheduling of networked microgrids using a resiliency index and robust optimization process that considered the market price and intermittent electricity generation uncertainties. The proposed method reduced the shed load by about 78.36 % concerning the base case. Ref. [32] proposed an energy management framework for the optimal scheduling of networked microgrids to reduce the impact of external shocks. The method minimized the operational costs considering the privacy of consumers. The demand response procedure decreased the shed load by about 57.3 % concerning the base case. Ref. [33] evaluated a resilient optimization process to cluster the system into multi-microgrids in external shock conditions. The energy loss, energy not supplied, voltage deviations, and reactive power not supplied were considered. The Pareto optimality method was utilized to find the best solution. Ref. [34] proposed a resilient scheduling algorithm for networked microgrids using a resiliency index. The analytical hierarchical algorithm calculated the resiliency index and the results indicated that the resiliency index was increased by about 25.38 % concerning the base case. Ref. [35] evaluated an optimization framework to determine the microgrid formation
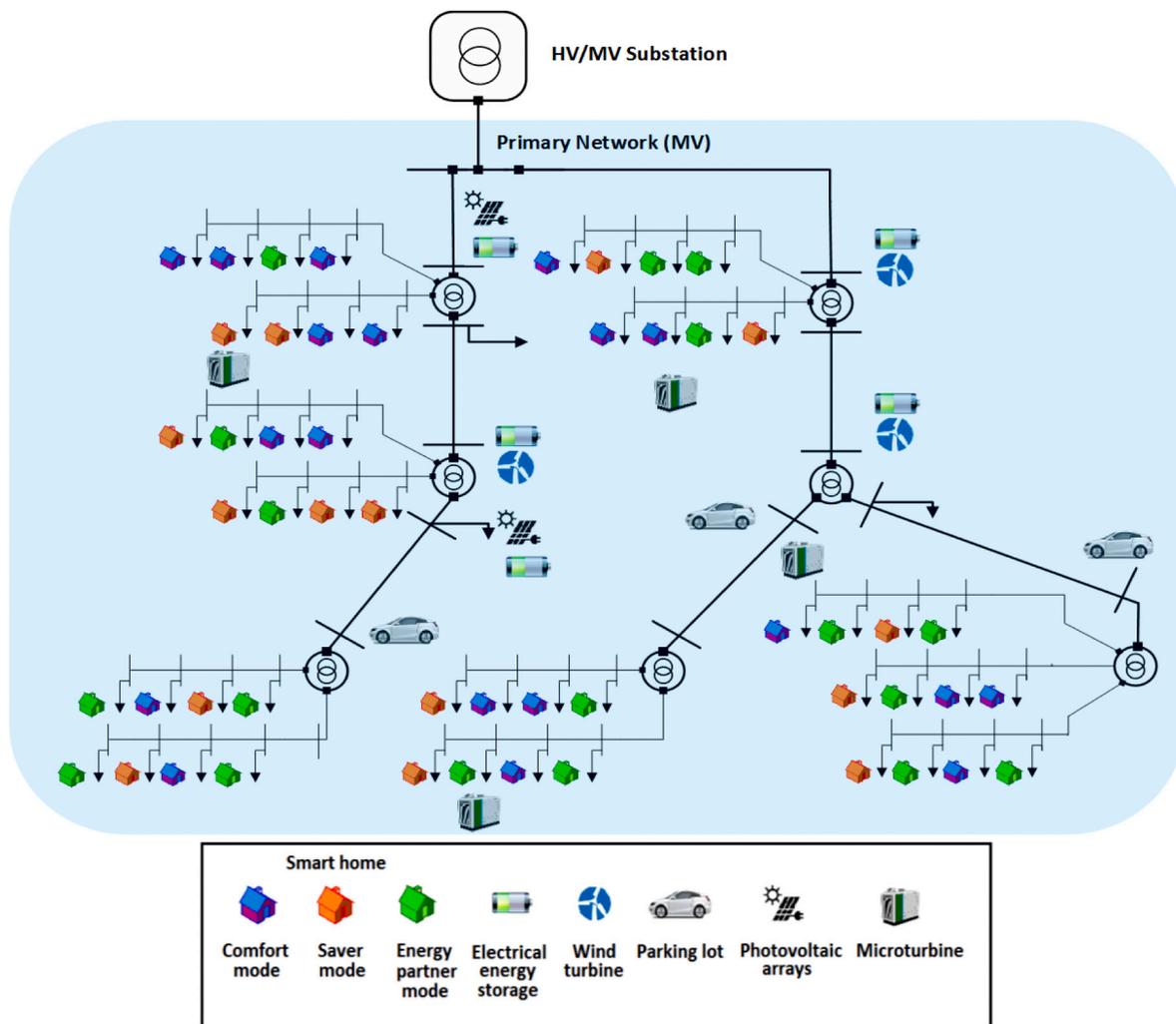
Fig. 1. Electrical distribution system with multiple distributed energy resources and smart homes.

of the distribution system and maximize the restored loads of the system. An iterative linear programming optimization model was utilized and the case study was performed for 33-bus IEEE and 69-bus PG&E systems. Ref. [36] assessed a three-stage resilient optimization algorithm that in the first stage, the hardening process of the system was performed. In the second stage, the switching process of the system was carried out and finally, in the third stage, the service restoration was optimized. Refs. [28–36] did not consider smart homes contribution modes, arbitrage opportunities, and locational marginal price in models. Further, Ref. [28–36] did not utilize the arbitrage index to explore the arbitrage process impacts on the scheduling of the distribution system.

Ref. [37] introduced a framework for optimal scheduling of active distribution networks considering the arbitrage strategies of distributed energy resources and aggregators. The model utilized a two-level optimization process for day-ahead and real-time horizons. The optimization process used robust and lexicographic ordering optimization methods. Ref. [37] did not consider the resilient operation of the distribution system, arbitrage index, locational marginal price modeling, and optimal resilient switching of the distribution system. Further, Ref. [37] did not model the smart homes categorization, contribution modes, and their arbitrage opportunities. Ref. [38] utilized the node resilience criteria to assess the impacts of hazards on the multi-infrastructure energy system. The model considered the interdependency of gas and electric networks and the load curtailment process was utilized using multiple scenarios. The performance of energy systems was explored considering the time-dependent performance of energy

generation and transmission facilities. Ref. [39] proposed a model to characterize the time dependency of renewable energy resources. A stochastic optimization process was used to optimize the dynamic microgrid formations. The model assessed the impacts of droop control and frequency regulation. The served critical load and frequency requirements of loads criteria were considered in the optimization process. Ref. [40] introduced a framework for simultaneously utilizing distributed energy resources and automated switches. The feasible network-based score method was developed to restore the critical loads of the system. A composite resiliency index was used to assess the effectiveness of the proposed process. Refs. [38–40] did not consider smart homes contribution modes and their arbitrage opportunities, locational marginal price, and optimal resilient switching of the distribution system. Further, Ref. [38–40] did not utilize the arbitrage index to assess the impacts of arbitrage of DERs on the scheduling of the distribution system.

An integrated framework that considers the impacts of the arbitrage process of smart homes on the optimal operational scheduling of resilient distribution system is less frequent in the literature. In this paper, an integrated framework for resiliency assessment of distribution system in the day-ahead and real-time horizons considering different modes of commitment of smart homes is proposed. The proposed model optimally dispatches the system energy resources considering arbitrage opportunities and resiliency of the system in the day-ahead and real-time markets.

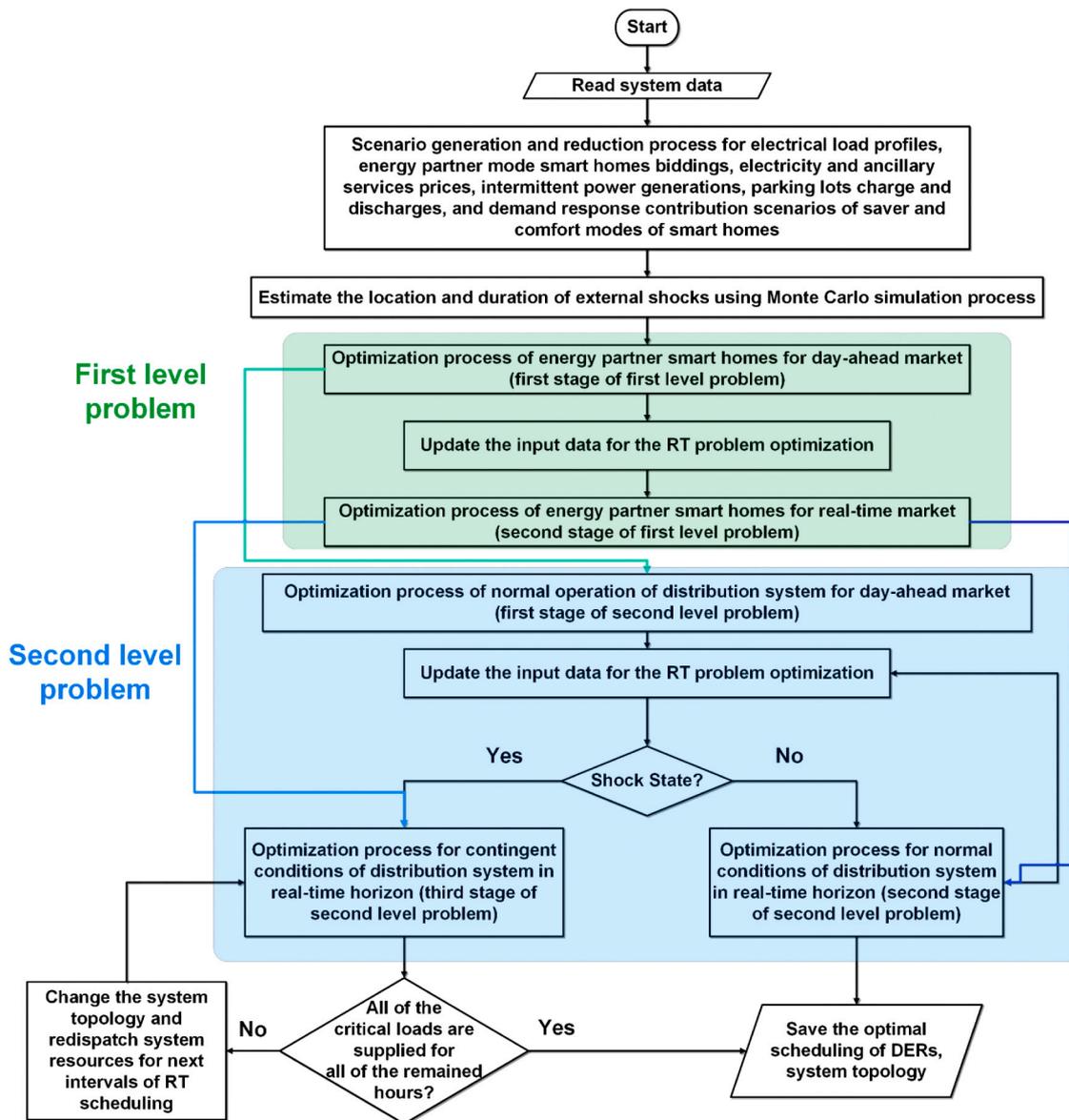The contributions of this paper are:

Fig. 2. The overall flowchart of the proposed procedure.

- The proposed model categorizes the smart homes into comfort, energy saver, and energy partner modes and the model considers a framework for optimizing the energy procurement from the smart homes dispatchable, non-dispatchable, and deferrable loads,
- The optimal bidding strategies of energy partner smart homes are simulated in the day-ahead and real-time markets considering their arbitrage opportunities,
- An arbitrage index is proposed that determines the smart homes arbitrage impacts on the distribution system operational cost,
- A resiliency index is proposed to assess the resiliency of the distribution system in day-ahead and real-time markets,
- The proposed algorithm determines the optimal scheduling of distribution system energy resources in normal and contingent conditions for the day-ahead and real-time horizons considering the arbitrage and resiliency indices,
- The algorithm minimizes the impacts of the external shocks contingencies using sectionalizing system into multi-microgrids and rescheduling of system resources.

The paper is organized as follows: The formulation of the problem is introduced in Section 2. In Section 3, the solution algorithm is presented.

In Section 4, the case study is presented. Finally, the conclusions are included in Section 5.

2. Problem modeling and formulation

As shown in Fig. 1, the distribution system utilizes IPGs, ESSs, microturbines, parking lots, and DRPs. Further, the distribution system imports electricity from the upward network in day-ahead and real-time horizons. Smart homes can contribute to demand response programs and deliver electricity to the distribution system in normal and external shock conditions. However, the arbitrage strategies of smart homes and their commitment scenarios may reduce the resiliency of the distribution system in external shock conditions. Thus, the distribution system should consider the impacts of arbitrage strategies of smart homes and their commitment scenarios on its scheduling process.

2.1. Smart home modeling

Smart homes may have photovoltaic panels, small wind turbines, energy management system electrical energy storage facilities, plug-in electric vehicles, and smart appliances [41]. The smart home
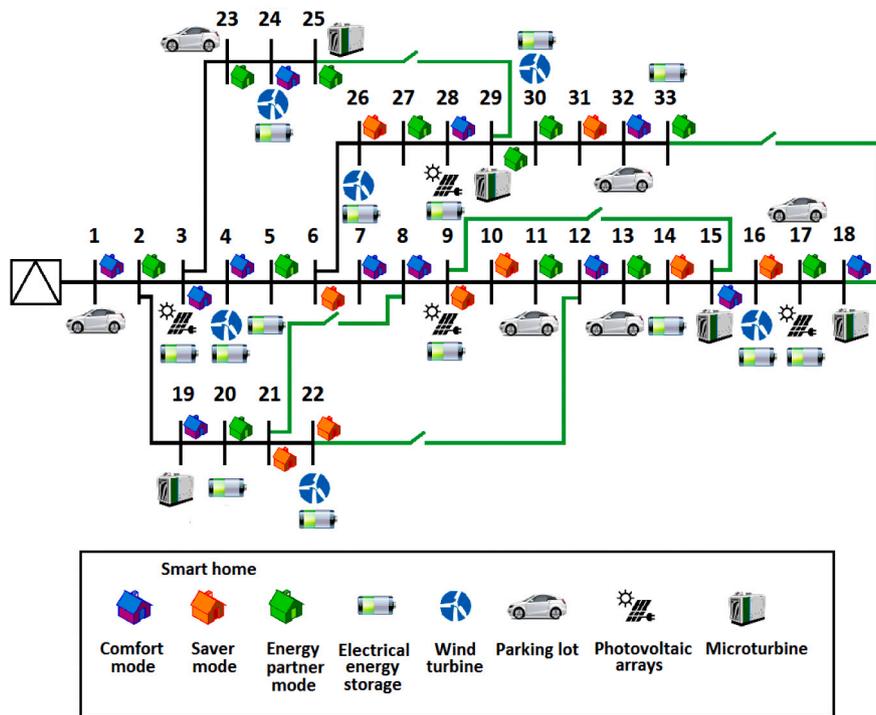
Fig. 3. The modified 33-bus IEEE test system.

Table 2
The location and capacity of distributed energy resources.

Type	Bus	Capacity (kW)
Photovoltaic system	3,9,17,28	60,60,40,50
Wind turbine	4,16,22,24,26,30	30,85,60,50,50,70

Table 3
The location and capacity of distributed energy resources.

#Microturbine	#Bus	C_{DS}^{DG} ($/kW)	P_{Max}^{DG} (kW)
1	15	0.095	800
2	18	0.093	650
3	19	0.085	100
4	25	0.098	750
5	29	0.099	750

Table 4
The scenario generation and reduction scenarios.

System parameter	Value
Number of solar irradiation scenarios	1000
Number of wind turbine power generation scenarios	1000
Number of PHEVs scenarios	1000
Number of demand response scenarios	1000
Number of day-ahead market load and price scenarios	1000
Number of real-time market load and price scenarios	1000
Number of energy partner smart homes bidding scenarios	1000
Number of solar irradiation reduced scenarios	10
Number of wind turbine power generation reduced scenarios	10
Number of PHEVs contribution reduced scenarios	10
Number of demand response contribution reduced scenarios	10
Number of day-ahead market load and price reduced scenarios	10
Number of real-time market load and price reduced scenarios	10
Number of energy partner smart homes bidding scenarios	10

appliances loads are categorized into dispatchable, non-dispatchable, and deferrable load groups. The non-dispatchable loads are 1) refrigerator, 2) lighting system and 3) entertainment system [41]. It is assumed that the non-dispatchable loads cannot be scheduled by the energy management system and they can be interrupted in contingent conditions. Further, their operation time cannot be transferred to another time.

The dispatchable loads are 1) air conditioning system, 2) PHEV, 3) electrical energy storage, and 4) water heaters with a thermal storage system. The dispatchable loads have predefined quantities considering the consumers' comfort levels and these quantities are continuously monitored by the energy management system. Thus, these loads can be controlled through a direct load control process without reducing the consumers' comfort levels.

The deferrable loads are 1) washing-drying machine and 2) oven. The deferrable load operation time is fixed and they cannot be interrupted during their operational time. The time-of-use demand response program is utilized by the distribution system operator to encourage smart homeowners to transfer the operation time of their deferrable

loads to other times. The distribution system receives data from the volume and duration of each smart appliance of the customer through the smart meter and the volume of non-dispatchable, dispatchable, and deferrable loads are known variables for the system operator. The customer can behave as prosumer and sell its energy and ancillary services to the distribution system [41].

Based on the above description, the customer operational modes can be categorized into the following groups from the distribution system viewpoint:

1) Comfort Mode of Smart Home (CMSH): the customer does not participate in demand response programs in normal conditions and the maximum value of the electrical load is considered as critical load. This type of customer prefers to maximize his/her comfort levels. Only for external shock conditions, the direct load control process is carried out and there is not any arbitrage scenario.

2) Saver Mode of Smart Home (SMSH): the customer fully participates in day-ahead and real-time demand response programs and the minimum value of the electrical load is considered a non-dispatchable load. This type of customer prefers to maximize his/her profits by
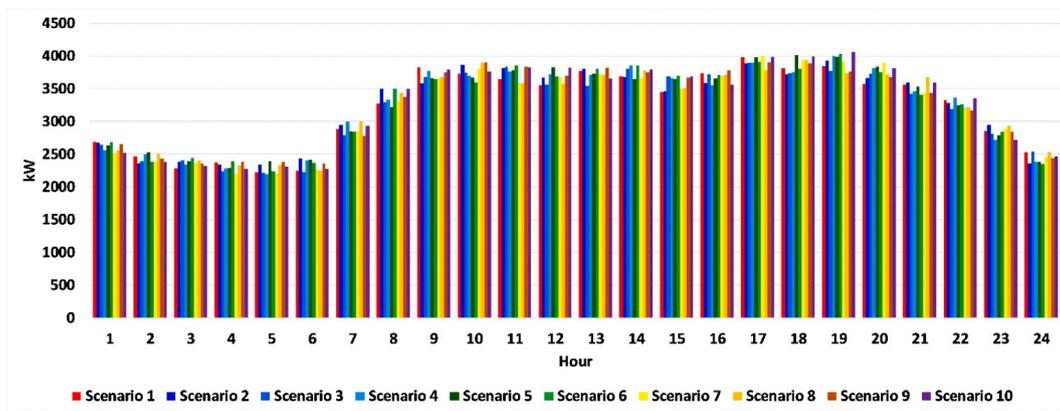
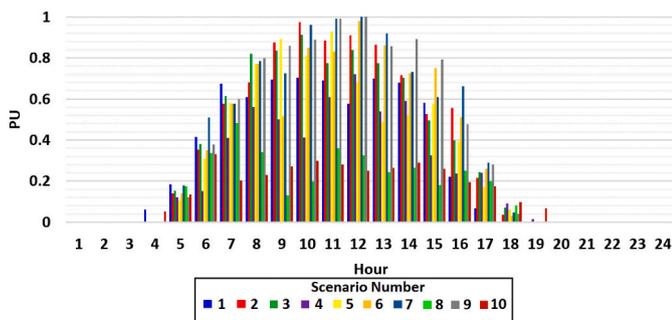**Fig. 4.** The day-ahead forecasted electrical load for the reduced scenarios.

Fig. 5. The forecasted photovoltaic electricity generation for one of the reduced scenarios.
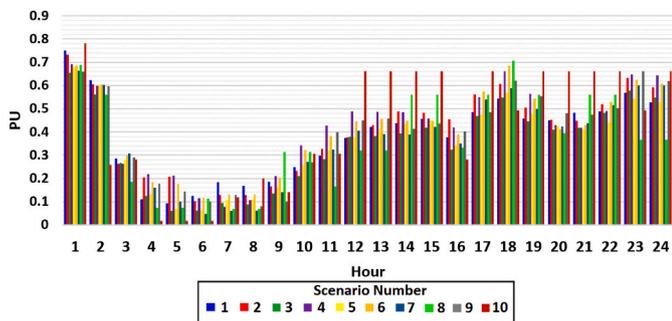

Fig. 6. The forecasted wind turbine electricity generation for one of the reduced scenarios.

participating in demand response programs. The direct load control and time of use process are fully allowed to carry out for their dispatchable and deferrable loads, respectively. There is not any arbitrage scenario for this type of customers.

3) Energy Partner mode of Smart Home (EPSH): the prosumer fully participates in day-ahead and real-time energy markets and demand response programs to transact energy and ancillary services with the distribution system. These prosumers perform the optimization process to participate in energy and ancillary markets and optimize their arbitrage opportunities. Further, the direct load control and time of use process are fully allowed to carry out for their dispatchable and deferrable loads, respectively. This type of smart home can deliver energy, reserve, and reactive power to the distribution system in the day-ahead market, meanwhile; they can deliver/purchase active power and reactive power to/from the distribution system in the real-time market. The

active and reactive power arbitrage can be performed by smart homes based on the fact that they can purchase electricity when the active power and/or reactive power prices are low and sell them when the prices of these services are high [42]. The arbitrage process can be implemented in both day-ahead and real-time markets. This process can highly increase the profit of smart homeowners and the energy procurement costs of the system. Further, this process has serious impacts on the distribution system resiliency in external shock conditions based on the fact that the scarcity of distributed energy resources may happen in the external shock conditions. The external shock may change the system topology and the distributed energy resources of the distribution system may not be available and dispatchable. Further, the energy partner smart homes may increase their bidding parameters, which may lead to higher values of locational marginal prices and energy procurement costs of the system. Thus, the distribution system should penalize them and reduce the arbitrage process of energy partner smart homes to increase the available dispatchable energy resources of its system.

2.2. Uncertainty modeling

The uncertainty of the following parameters is modeled in the optimization process using scenario generation/reduction of autoregressive integrated moving average model: energy partner mode smart homes biddings, electricity and ancillary services prices, electrical load profiles, intermittent power generations, parking lots charge and discharges, and demand response contribution scenarios of saver and comfort modes of smart homes [43–44]. Further, the Monte Carlo stochastic process is utilized to estimate the intensity and location of external shocks [44].

2.3. The proposed optimization framework

This paper presents a multi-level optimization process to assess the resiliency of the distribution system in the day-ahead and real-time horizons. The optimization process is decomposed into two levels that consist of optimal operational scheduling of smart homes and distribution system in the first and second levels, respectively. The first level problem consists of two stages of the optimization process for optimal operational scheduling of smart homes in the day-ahead and real-time horizons, respectively. Then, the outputs of the first-level optimization problem are delivered to the second-level optimization procedure. The second level problem consists of three stages of optimization problems for operational scheduling of distribution system in normal and contingent conditions.

At the first stage of the second level problem, the DSO determines the day-ahead optimal scheduling of distributed energy resources in the normal conditions of its system. At the second stage of the second level problem, the DSO optimizes the real-time operational scheduling of the
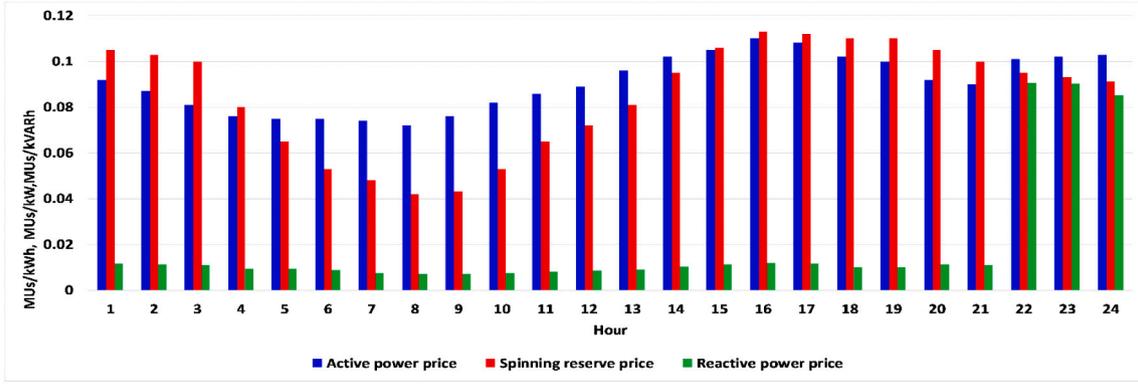
Fig. 7. The forecasted day-ahead electricity and ancillary services prices for one of the reduced scenarios.
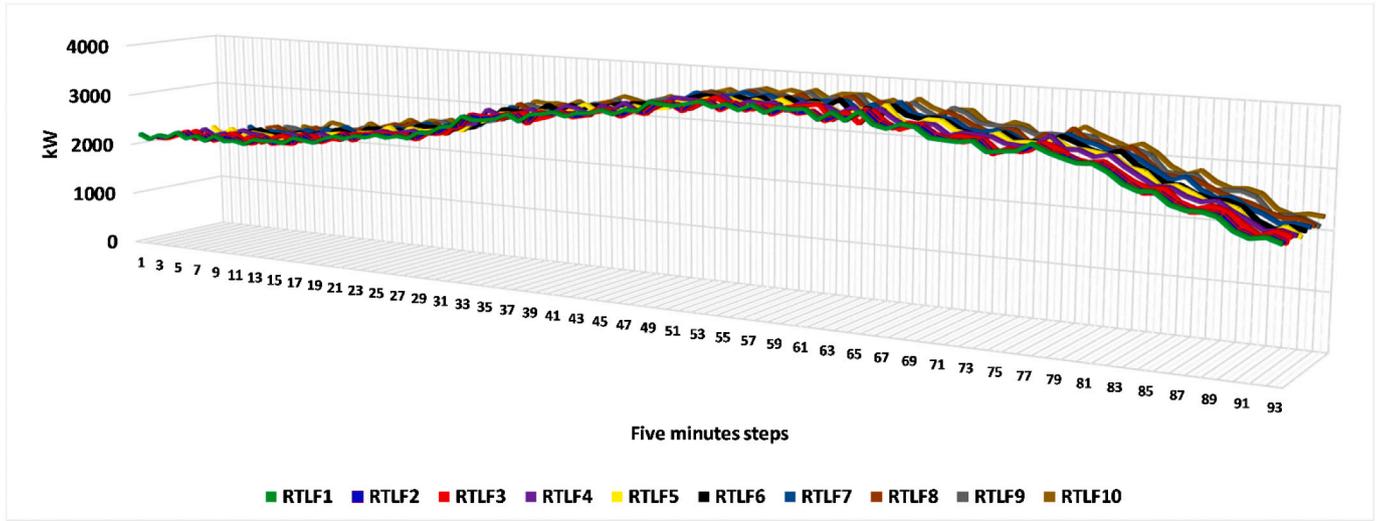

Fig. 8. The forecasted load of the system in the real-time horizon for 5 min forecasting intervals.

system. Finally, in the third stage of the second level problem, the DSO explores the impacts of external shocks on its systems, optimizes the system topology, and redispatches its resources.

2.4. Energy partner smart homes optimal bidding strategies in the day-ahead market (first stage of first level problem)

The smart home can submit its energy, reserve, and reactive power to the distribution system in the day-ahead market. Thus, the objective function of the first stage of the first level problem is the maximization of smart homes profits for the day-ahead electricity market, which can be written as (1):

The objective function is divided into ten terms: 1) the cost of smart home intermittent power generation ($C_{SH}^{IPG\ DA}$); 2) the cost of smart home fossil-fueled distributed generation ($C_{SH}^{DG\ DA}$); 3) the cost of smart home energy storage system ($C_{SH}^{ESS\ DA}$); 4) the cost of smart home PHEV ($C_{SH}^{PHEV\ DA}$); 5) the smart home energy purchasing cost ($C_{SH}^{Purchase\ DA}$); 6) the smart home benefit of energy and ancillary services sold to the distribution system ($B_{SH}^{Sell\ DA}$); 7) the smart home benefit of demand response programs ($B_{SH}^{DRP\ DA}$); 8) the smart home benefit of energy and ancillary services arbitrage ($B_{SH}^{AR\ DA}$); 9) the smart home active power mismatch penalties ($\sum Penalty^{active\ DA}$); and 10) the smart home reactive power mismatch penalties ($\sum Penalty^{reactive\ DA}$).

The smart home revenue in the day-ahead market can be written as (2):

$$Max\ \mathbb{F}_{DA}^{SH} = \sum_{t=1}^{24} \sum_{NSHOS} Prob. \begin{pmatrix} -C_{SH}^{IPG\ DA} - C_{SH}^{DG\ DA} - C_{SH}^{ESS\ DA} - C_{SH}^{PHEV\ DA} - C_{SH}^{Purchase\ DA} + \\ B_{SH}^{Sell\ DA} + B_{SH}^{DRP\ DA} + B_{SH}^{AR\ DA} - \sum Penalty^{active\ DA} - \sum Penalty^{reactive\ DA} \end{pmatrix} \qquad (1)$$
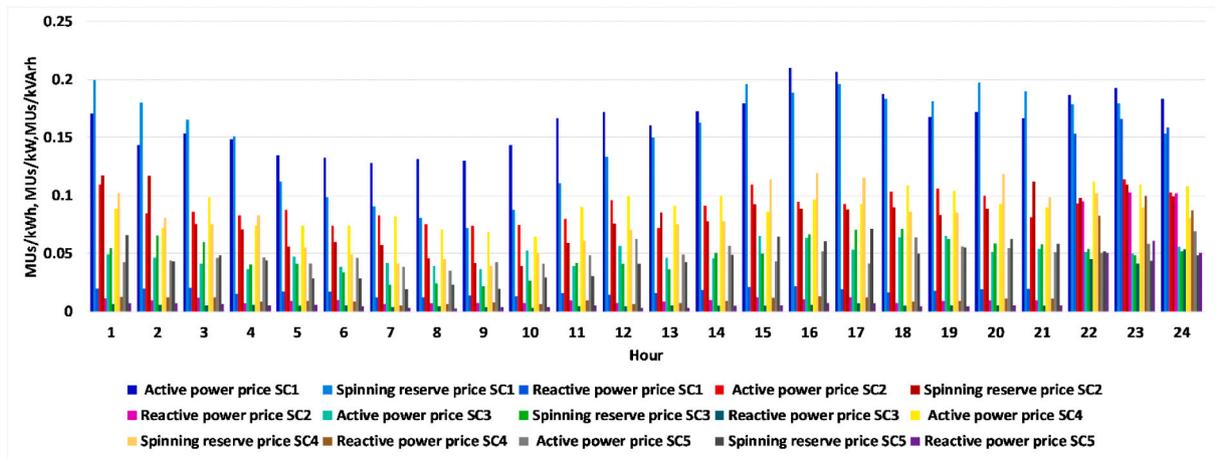
(a)
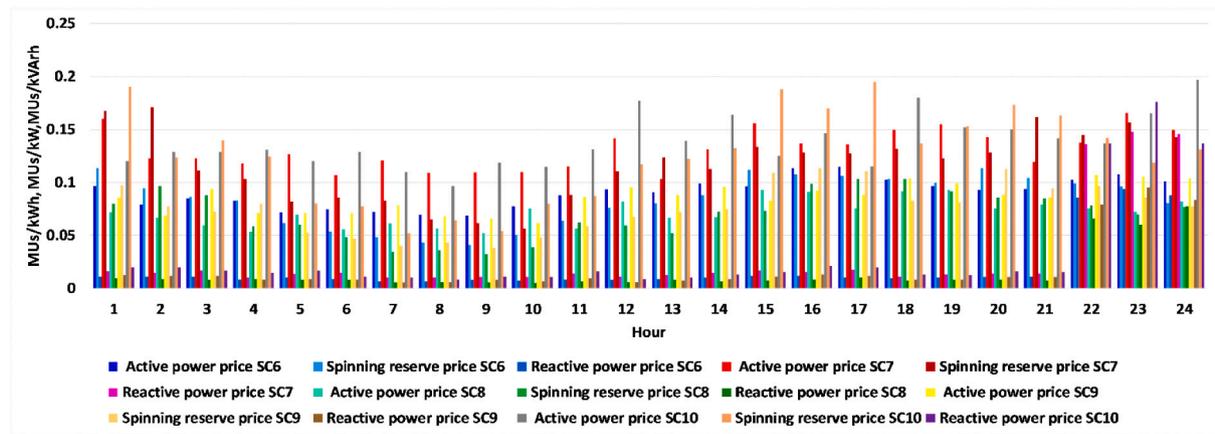
(b)

Fig. 9. (a) The average hourly values of forecasted real-time electricity and ancillary services prices for scenarios 1–5, (b) The average hourly values of forecasted real-time electricity and ancillary services prices for scenarios 6–10.

$$B_{SH}^{Sell\ DA} = \left(\sum \xi^{SR} \cdot SR_{DA}^{SH} + \sum \xi^{active} \cdot P_{DA}^{SH} + \sum \xi^{reactive} \cdot Q_{DA}^{SH} \right) \tag{2}$$

Eq. (2) decomposes into the following terms: the profit of smart home spinning reserve sold to the distribution system in the day-ahead market ($\sum \xi^{SR} \cdot SR_{DA}^{SH}$), the profit of smart home active power sold to the distribution system for the day-ahead market ($\sum \xi^{active} \cdot P_{DA}^{SH}$), and the profit of smart home reactive power sold to the distribution system in the day-ahead market ($\sum \xi^{reactive} \cdot Q_{DA}^{SH}$).

The smart home optimization objective function for the day-ahead horizon has the following constraints:

A. Electrical power balance constraint:

$$Q_{SH}^{Total} = \left(\sum Q_{SH}^{DG} + \sum Q_{SH}^{DRP} - \sum Q_{SH}^{Load} - Q_{AMG}^{Loss} \pm \sum Q_{SH}^{PHEV} \right) \tag{4}$$

Eq. (3) terms are the intermittent and distributed generation power generation active power injections to the distribution system ($\sum P_{SH}^{IPG} + \sum P_{SH}^{DG}$), the active power injection/ withdrawal of energy storage ($\sum P_{SH}^{ESS}$), the active power injection of demand response program ($\sum P_{SH}^{DRP}$), the active power injection/withdrawal ($\sum P_{SH}^{PHEV}$), the active power consumption of load ($\sum P_{SH}^{Load}$), and active power loss ($\sum P_{SH}^{Loss}$).

Eq. (4) terms are the distributed generation power generation reac-

$$P_{SH}^{Total} = \left(\sum P_{SH}^{IPG} + \sum P_{SH}^{DG} \pm \sum P_{SH}^{ESS} + \sum P_{SH}^{DRP} \pm \sum P_{SH}^{PHEV} - \sum P_{SH}^{Load} - \sum P_{SH}^{Loss} \right) \tag{3}$$
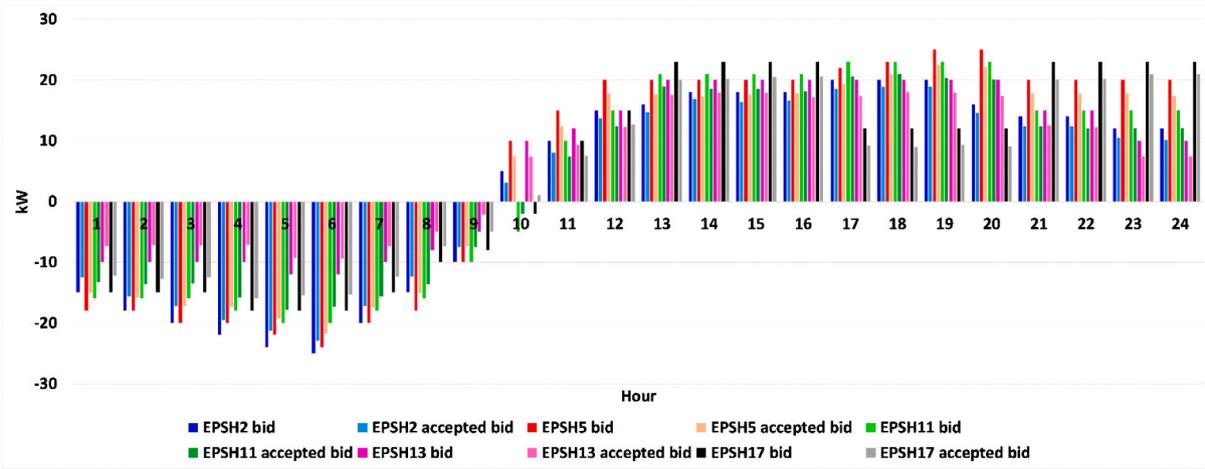
(a)
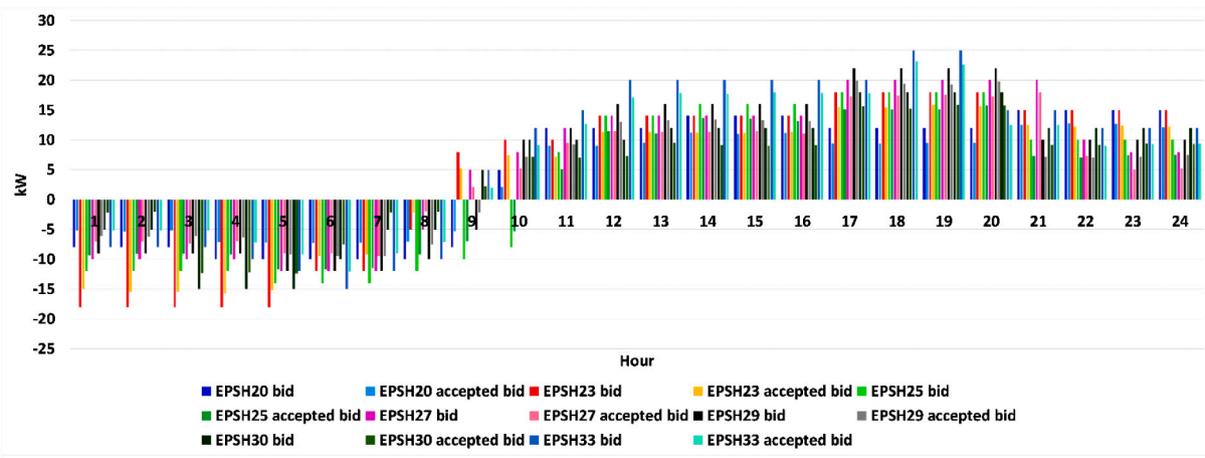
(b)

Fig. 10. (a) The day-ahead active power bidding and their accepted values of EPSH (2, 5, 11, 13, 17), (b) The day-ahead active power bidding and their accepted values of EPSH (20, 23, 25, 27, 29, 30, 33).

tive power injection to the distribution system ($\sum Q_{SH}^{DG}$), the demand response program reactive power injection ($\sum Q_{SH}^{DRP}$), the reactive power withdrawal of load ($\sum Q_{SH}^{Load}$), reactive power loss (Q_{SH}^{Loss}), and reactive power injection/withdrawal of PHEV ($\sum Q_{SH}^{PHEV}$).

B. Demand response constraints:

The smart home loads consist of dispatchable, non-dispatchable, and deferrable loads that can be written as (5–11):

$$P_{SH}^{Load} = P_{SH\ Dispatchable}^{Load} + P_{SH\ Deferrable}^{Load} + P_{SH\ Non-dispatchable}^{Load} \tag{5}$$

$$\Delta P_{SH}^{TOU} = P_{SH\ Deferrable}^{Load} \tag{6}$$

$$\sum_{t=1}^{T} \Delta P_{SH}^{TOU} = 0 \tag{7}$$

$$\Delta P_{SH\ Max}^{DLC} = P_{SH\ Dispatchable}^{Load} \tag{8}$$

$$P_{SH}^{DRP} = \Delta P_{SH}^{DLC} + \Delta P_{SH}^{TOU} \tag{9}$$

$$\Delta P_{SH\ Min}^{DLC} \leq \Delta P_{SH}^{DLC} \leq \Delta P_{SH\ Max}^{DLC} \tag{10}$$

$$\Delta P_{SH\ Min}^{TOU} \leq \Delta P_{SH}^{TOU} \leq \Delta P_{SH\ Max}^{TOU} \tag{11}$$

Eq. (5) terms are the smart home dispatchable load ($P_{SH\ Dispatchable}^{Load}$),

deferrable load ($P_{SH\ Deferrable}^{Load}$), and non-dispatchable load ($P_{AMG\ Dispatchable}^{Load}$), respectively [45]. Eq. (6) presents that the maximum value of time-of-use change in electrical loads is equal to deferrable load. Eq. (7) presents that time-of-use changes in loads should equal zero in the day-ahead horizon based on the fact that the deferrable loads should be supplied through the optimization interval [45]. Eq. (8) presents that the maximum value of direct load control is equal to dispatchable load. Eq. (9) terms are the sum of the changes of direct load control and time-of-use active powers based on the fact that the demand response process can be implemented through direct load control and time-of-use procedures [45]. Eq. (10) and Eq. (11) are the limits of direct load control and time-of-use active powers, respectively [45].

The PHEV model and constraints are available in [45] and are not presented for the sack of space.

2.5. Energy partner smart homes optimal bidding strategies in the real-time market (second stage of first level problem)

The second stage of the first level problem maximizes the profit of smart home resources in the RT market. The objective function of this problem can be represented as (12):

The objective functions of (12) terms are the same as (1). However,
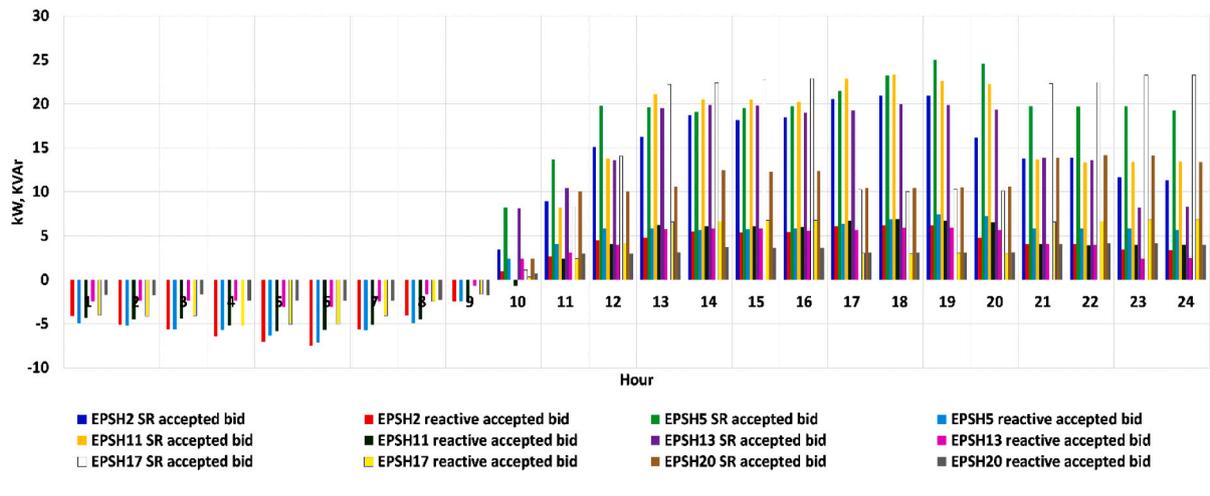
(a)
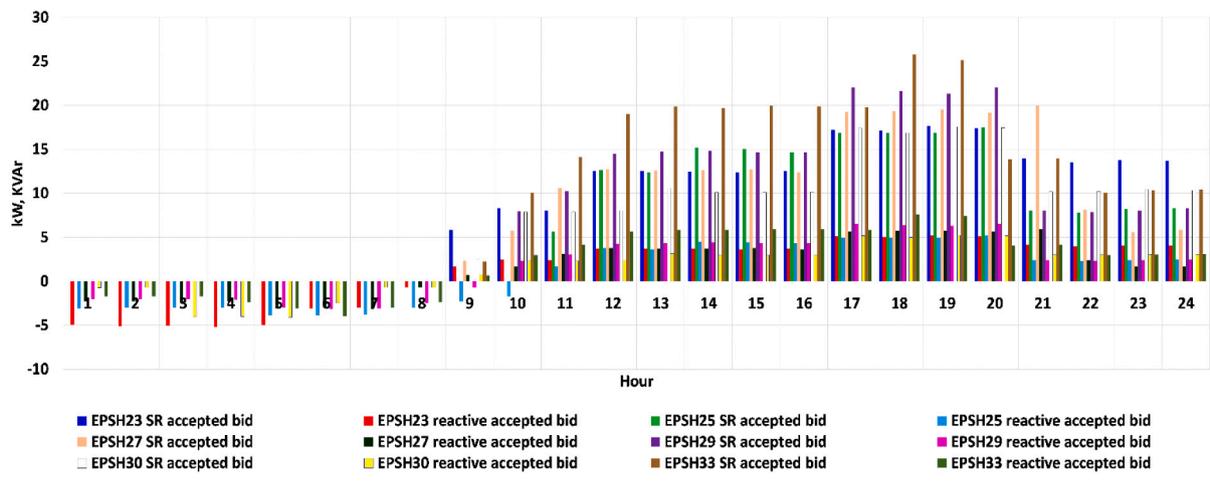
(b)

Fig. 11. (a) The day-ahead reactive power and spinning reserve bidding and accepted values of EPSH (2, 5, 11, 13, 17, 20), (b) The day-ahead reactive power and spinning reserve bidding and accepted values of EPSH (23, 25, 27, 29, 30, 33).
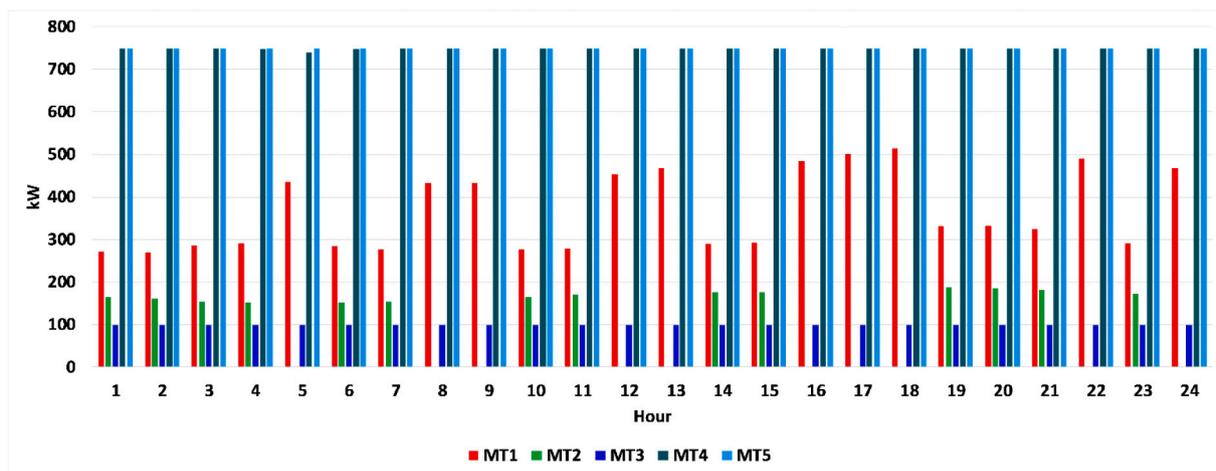
Fig. 12. The estimated values of day-ahead active generations of microturbines for one of the reduced scenarios.
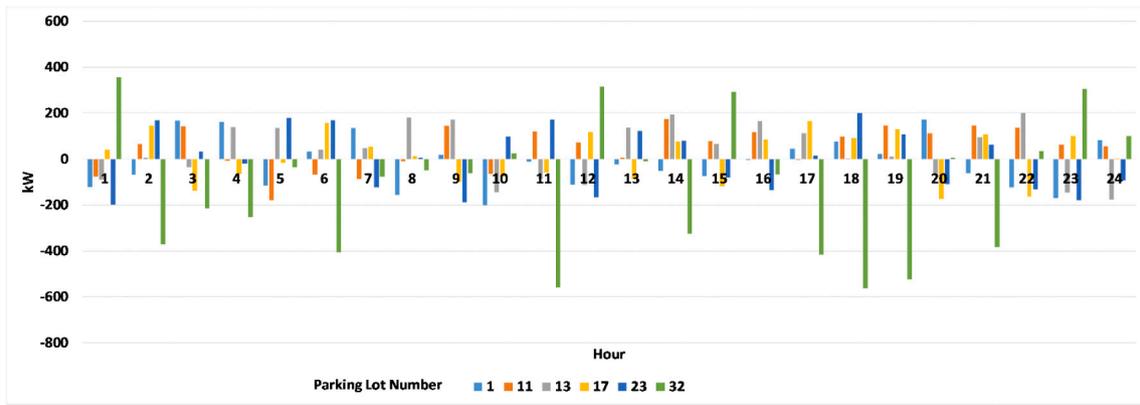
Fig. 13. The estimated values of day-ahead electricity transactions of PHEV parking lots for one of the reduced scenarios.
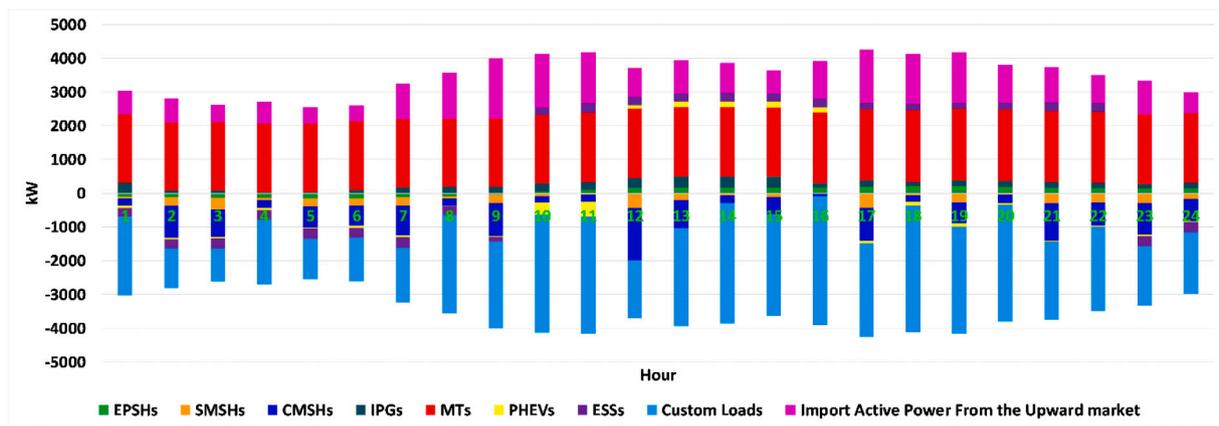
Fig. 14. The distributed energy resources and smart homes electricity transactions for the day ahead optimization interval.
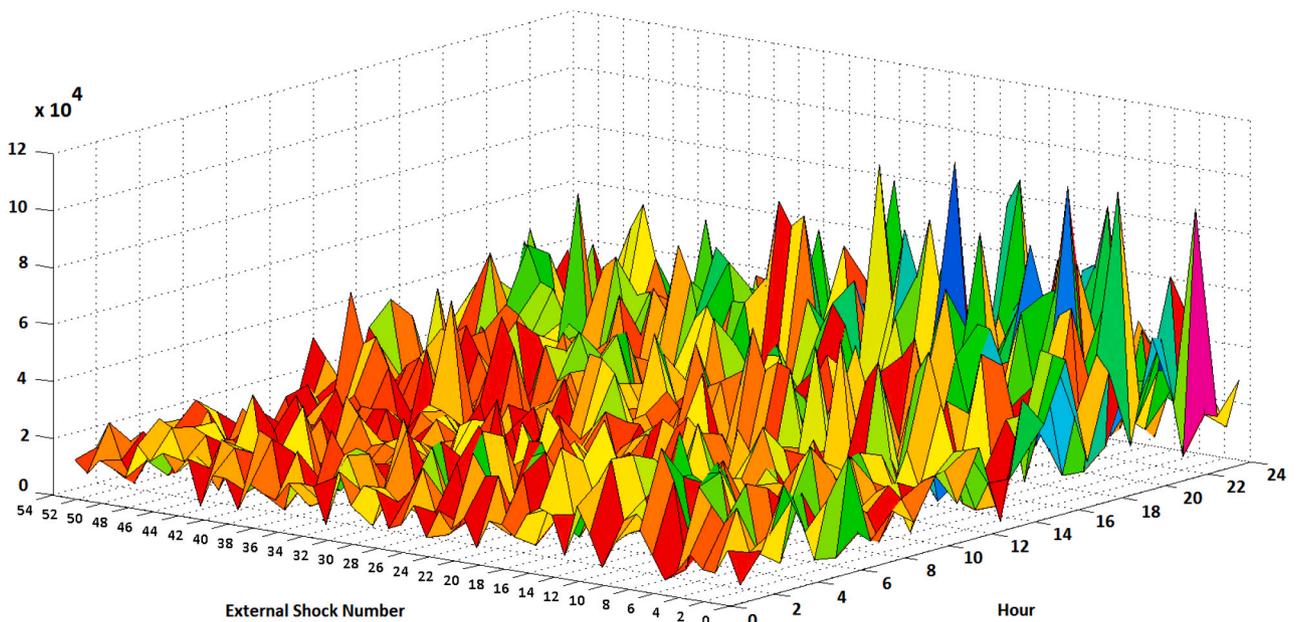
Fig. 15. The aggregated expected operational and energy not supplied costs for the 54 most credible external shocks and day-ahead optimization horizon.
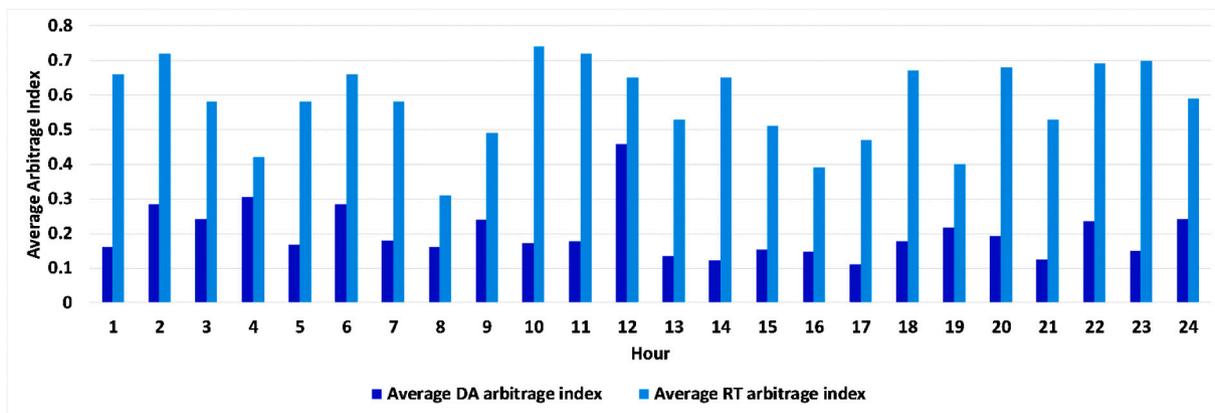
Fig. 16. The estimated values of the average hourly arbitrage index for the day-ahead and real-time optimization horizons.
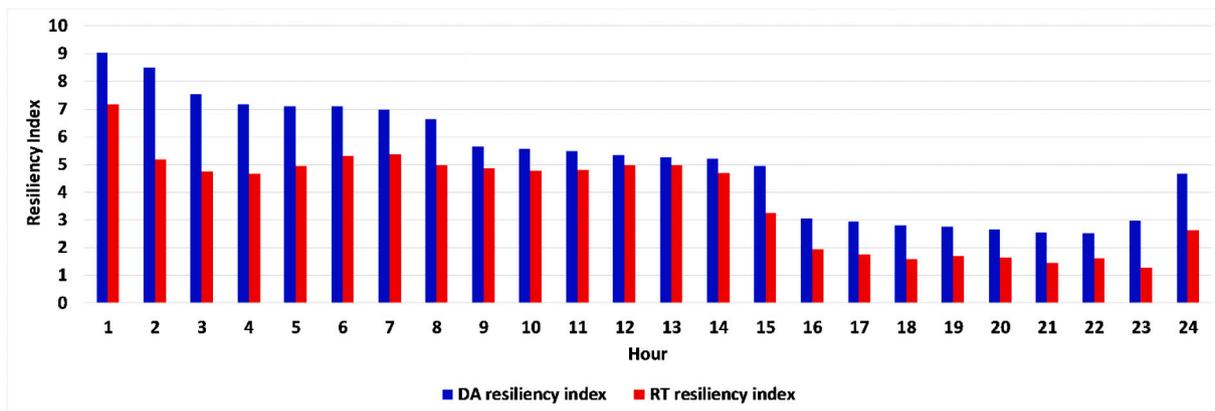
Fig. 17. The estimated values of the average hourly resiliency index for the day-ahead and real-time optimization horizons without implementing the proposed method.
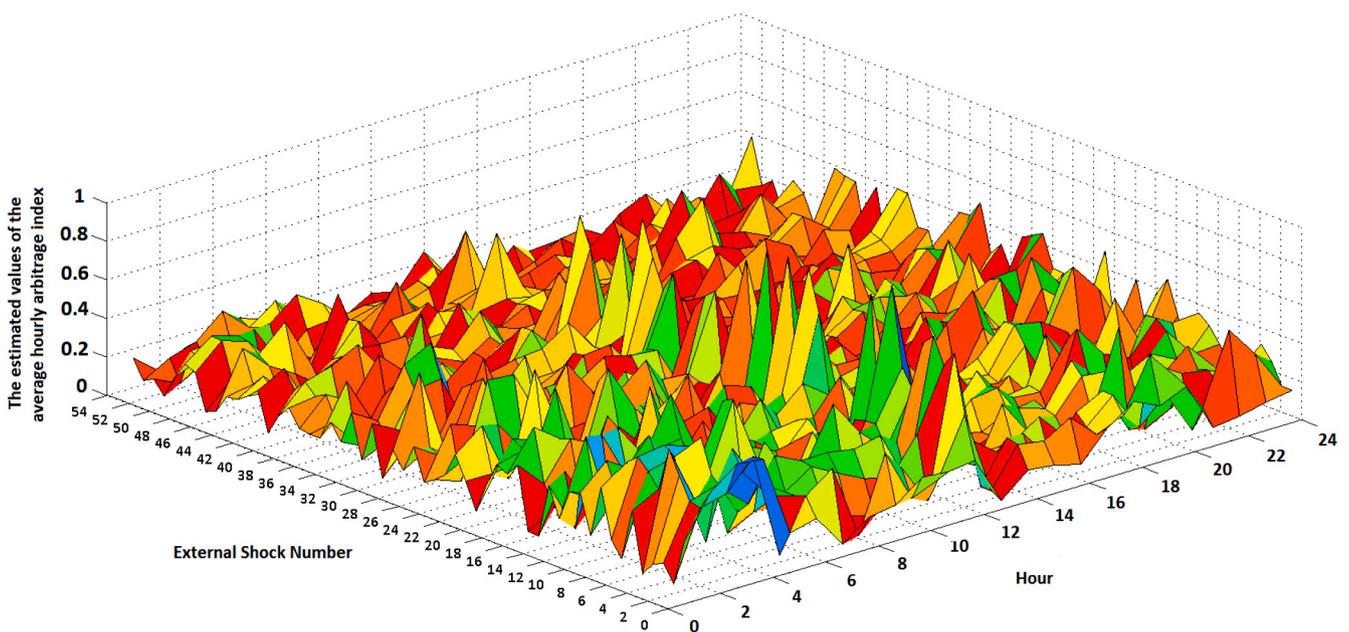
Fig. 18. The estimated values of the average hourly arbitrage index for the 54 most credible external shocks and day-ahead optimization horizon.
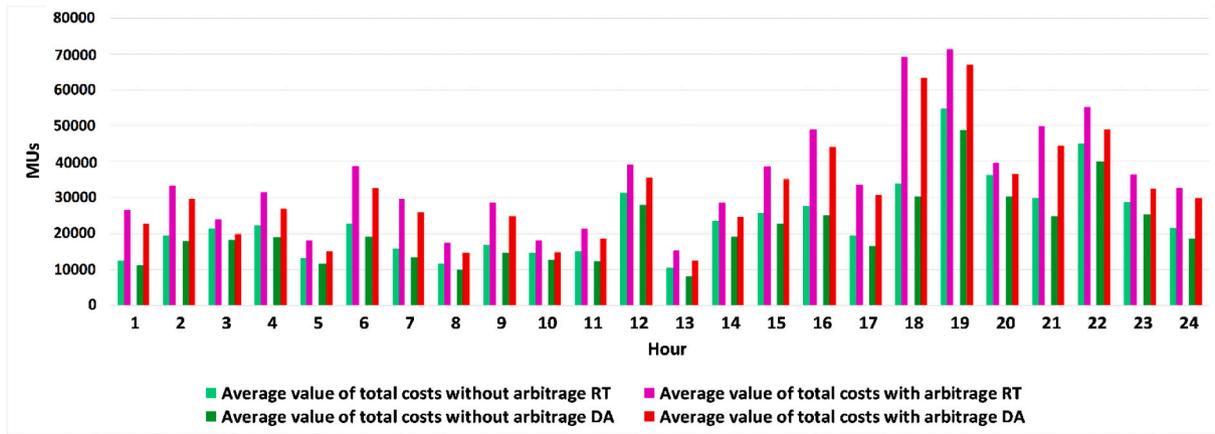
Fig. 19. The estimated values of operational costs of the system for the day-ahead and real-time optimization horizons with and without the arbitrage process of smart homes.
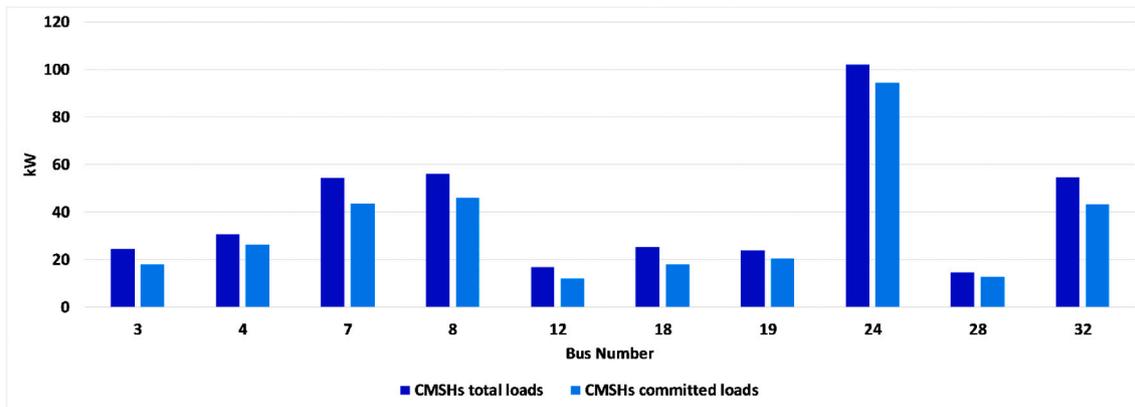
(a)
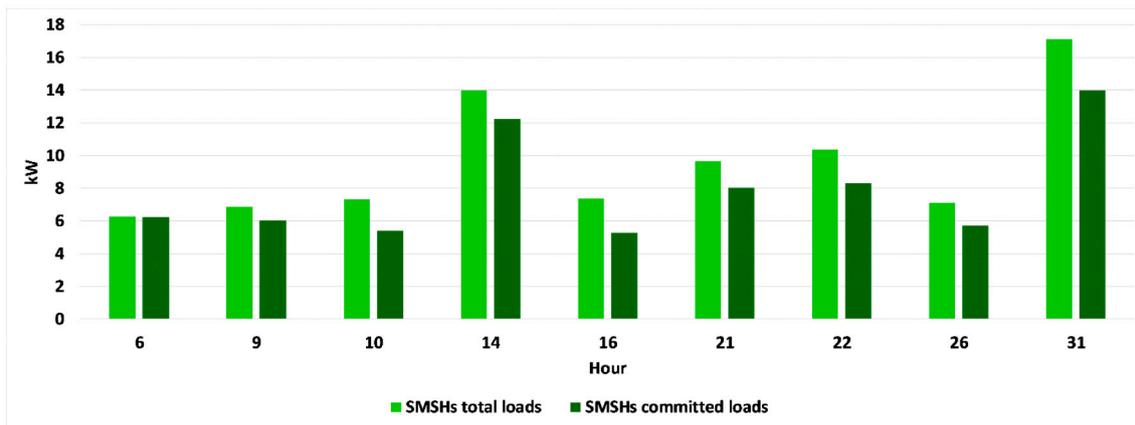
(b)

Fig. 20. (a) The value of load commitment of CMSHs, (b) the value of load commitment of SMSHs.

$$Max\ \mathbb{F}_{RT}^{SH} = \sum_{t=k}^{k+1} \begin{pmatrix} -C_{SH}^{IPG\ RT} - C_{SH}^{DG\ RT} - C_{SH}^{ESS\ RT} - C_{SH}^{PHEV\ RT} - C_{SH}^{Purchase\ RT} + \\ B_{SH}^{Sell\ RT} + B_{SH}^{DRP\ RT} + B_{SH}^{AR\ RT} - \sum Penalty^{active\ RT} - \sum Penalty^{reactive\ RT} \end{pmatrix} \qquad (12)$$
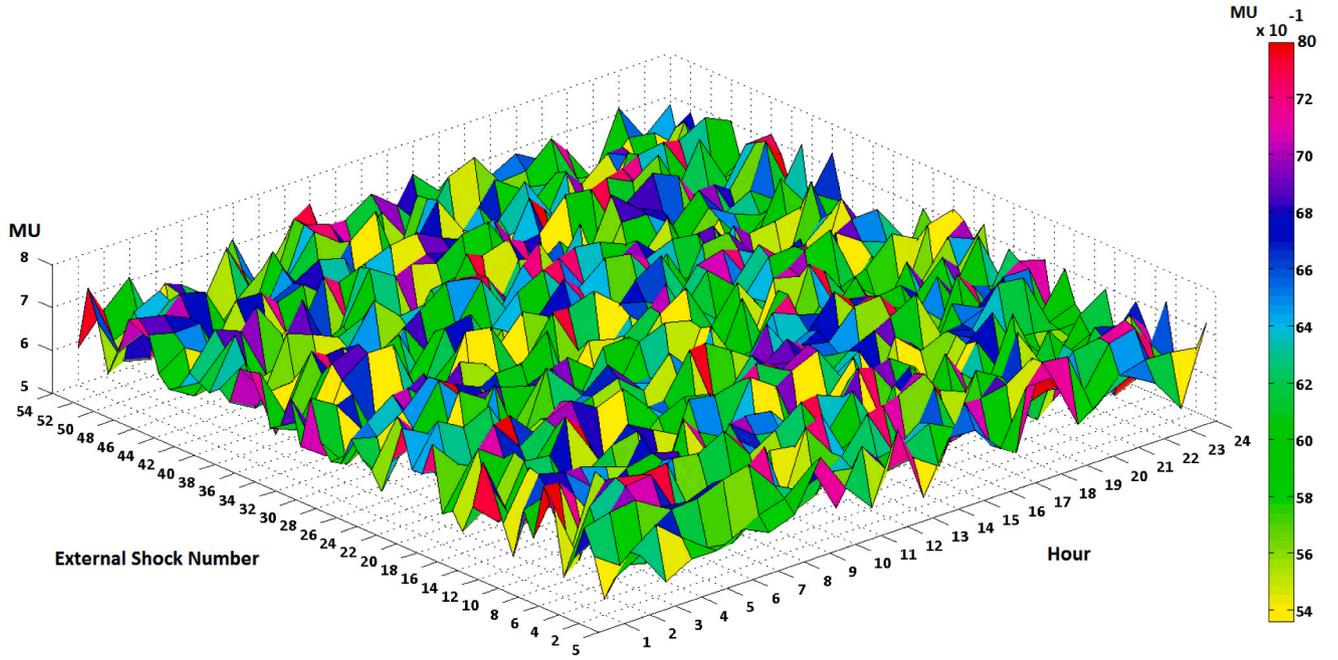
Fig. 21. The estimated values of the highest value of locational marginal of the system for external shocks considering the arbitrage process of smart homes.

the optimization process is carried out for 15 min snapshots.

The smart home revenue in the real-time market can be written as (13):

$$B_{SH}^{Sell\ RT} = \left(\sum \gamma^{active} \cdot P_{RT}^{SH} + \sum \gamma^{reactive} \cdot Q_{RT}^{SH} \right) \tag{13}$$

Eq. (13) terms are the smart home active power sold to the distribution system for the real-time market ($\sum \gamma^{active} \cdot P_{RT}^{SH}$), and the smart home reactive power sold to the distribution system in the real-time market ($\sum \gamma^{reactive} \cdot Q_{RT}^{SH}$).

The smart home optimization objective function for the real-time horizon has the same constraints as the day-ahead optimization process.

- The day-ahead dispatching of the system distributed energy resources, dispatchable and deferrable loads of saver mode of smart homes, and energy partner mode of smart homes distributed energy resources,
- Penalizing smart homes that utilize arbitrage strategy for the day-ahead horizon,
- Changing the time-of-use and direct load control fees for the day-ahead horizon.

The objective functions of the first stage of the second level problem are the maximization of profits of the distribution system for the day-ahead operational horizon that can be written as (14):

$$Max\ \mathbb{Z}_{DS}^{DA} = \sum_{t=1}^{24} \sum_{NDSDA} prob. \begin{pmatrix} W_1 \cdot \left(-C_{DS}^{IPG\ DA} - C_{DS}^{DG\ DA} - C_{DS}^{ESS\ DA} - C_{DS}^{PLOT\ DA} - C_{DS}^{Purchase\ DA} - \\ ENSC + B_{DS}^{Sell\ DA} - C_{DS}^{DRP\ DA} - C_{DS}^{AR\ DA} + \sum Penalty^{active\ DA} + \\ \sum Penalty^{reactive\ DA} \right) + W_2 \cdot RI - W_3 \cdot \sum_{NB} LMP - W_4 \cdot \sum_{NDSRT} prob. \mathbb{Z}_{DS}^{RT} \end{pmatrix} \tag{14}$$

2.6. Optimal operation of distribution system in day-ahead normal conditions (first stage of second level problem)

The distribution system receives the smart homes' bids for the next 24 h and optimizes the scheduling of its distributed energy resources using the unit commitment process. The distribution system operator can reject the smart home bids that utilize the arbitrage strategy and penalize them. Further, the distribution system can schedule the demand response programs that consist of direct load control and time-of-use processes.

Thus, the day-ahead system control variables can be categorized into the following groups:

The objective function is divided into fourteen terms: 1) the cost of distribution system intermittent power generation ($C_{DS}^{IPG\ DA}$); 2) the cost of distribution system distributed generation ($C_{DS}^{DG\ DA}$); 3) the cost of distribution system energy storage system ($C_{DS}^{ESS\ DA}$); 4) the cost of distribution system PHEV parking lots ($C_{DS}^{PLOT\ DA}$); 5) the distribution system energy cost purchased from the upward market ($C_{DS}^{Purchase\ DA}$); 6) the energy not supplied costs (*ENSC*); 7) the benefit of energy sold to the smart homes ($B_{DS}^{Sell\ DA}$); 8) the cost of demand response programs ($C_{DS}^{DRP\ DA}$); 9) the cost of energy and ancillary services arbitrage imposed by smart homes ($C_{DS}^{AR\ DA}$); 10) the benefit of smart homes active power mismatch penalties ($\sum Penalty^{active\ DA}$); 11) the benefit of smart homes reactive power mismatch penalties ($\sum Penalty^{reactive\ DA}$); 12) the resiliency index; 13) the sum of the locational marginal price of system

Table 5
The number of switching of switches to restore the system from external shock impacts.

Ext. Shock	1	2	3	4	5	6	7	8	9	10	11	12	13	14	15	16	17	18	19	20	21	22	23	24
1	4	4	5	4	4	6	4	6	5	5	4	6	4	4	4	4	4	5	4	4	3	3	4	4
2	4	5	6	5	5	6	5	5	3	3	4	6	4	4	6	6	5	6	5	6	6	3	5	4
3	4	5	4	6	5	5	5	5	6	6	5	4	3	6	4	5	4	5	6	3	6	3	4	5
4	5	5	4	5	5	4	3	5	5	5	4	3	4	5	4	5	4	6	4	4	6	6	5	5
5	3	4	4	5	4	5	6	5	5	5	4	4	4	4	5	4	4	5	3	6	3	4	4	4
6	6	5	4	4	4	3	3	5	4	4	5	3	5	8	5	3	5	4	6	5	3	6	4	4
7	5	4	3	4	4	6	3	5	3	6	4	5	5	3	4	5	3	4	5	5	4	5	4	4
8	4	5	5	5	3	6	3	3	4	4	4	5	4	5	5	4	5	5	5	5	5	4	4	5
9	4	5	6	4	5	5	4	4	5	4	4	4	5	3	4	4	6	5	5	5	6	3	4	5
10	4	5	6	6	5	5	5	5	6	5	5	5	3	4	5	5	5	6	3	4	4	3	3	4
11	3	4	5	3	5	5	6	3	3	4	5	5	5	4	4	3	5	4	4	5	5	3	6	4
12	3	4	5	4	4	3	3	6	3	5	4	4	5	5	6	3	6	3	4	6	5	5	4	4
13	5	6	3	5	4	5	3	3	4	4	3	5	3	5	5	3	5	4	4	4	5	4	5	3
14	4	5	5	3	6	5	3	4	4	3	3	4	4	5	5	4	3	5	4	5	3	6	6	5
15	5	4	4	4	4	6	5	5	6	5	3	4	3	4	4	4	5	5	4	4	4	4	4	6
16	5	6	4	6	3	4	5	4	6	4	6	7	6	5	5	6	5	8	4	3	4	6	6	5
17	5	5	5	3	3	4	6	5	5	4	4	5	5	3	5	5	3	4	6	6	4	5	4	4
18	4	6	6	4	5	4	5	3	4	3	4	3	4	4	4	4	5	4	4	4	5	4	5	3
19	6	5	4	5	4	3	3	5	4	6	4	3	4	5	4	3	5	4	6	4	4	5	3	5
20	6	6	3	4	3	5	6	3	5	4	4	4	4	3	4	6	4	5	5	4	3	6	5	6
21	3	5	5	3	5	5	5	4	5	5	4	5	4	4	3	4	5	5	6	5	5	3	4	4
22	3	6	5	4	5	4	5	6	6	4	5	5	5	4	5	6	6	4	5	5	4	4	3	4
23	6	5	5	4	3	3	5	4	4	3	3	5	4	4	4	6	4	5	3	5	6	5	4	4
24	4	5	4	4	4	7	4	4	4	6	4	3	5	4	4	3	4	4	3	5	5	4	4	6
25	4	5	5	3	4	4	6	4	4	3	4	6	4	5	4	4	5	4	7	4	4	5	5	6
26	4	5	4	5	6	5	5	6	3	5	4	5	3	5	3	6	5	5	5	4	5	6	4	4
27	6	5	5	5	4	5	4	6	4	4	5	3	4	4	5	5	5	5	5	4	5	4	5	5
28	5	4	3	4	5	5	4	4	4	5	6	5	3	5	6	6	4	6	6	5	4	6	4	5
29	5	5	4	4	5	5	4	5	5	4	3	3	3	5	5	4	5	5	3	3	6	4	4	4
30	4	5	3	5	3	5	4	4	4	4	4	5	5	4	8	3	5	5	6	6	3	4	4	5
31	4	3	4	5	4	4	5	5	4	3	4	4	4	3	3	3	4	5	4	5	6	5	5	4
32	4	4	3	5	5	4	3	3	4	7	5	5	5	5	5	4	4	3	3	3	5	4	4	5
33	3	4	5	4	4	4	4	5	5	4	5	3	5	4	6	5	5	4	4	4	6	4	5	4
34	5	6	7	3	6	5	6	3	3	3	4	6	4	5	6	5	4	5	3	5	4	4	4	3
35	4	5	5	5	4	4	5	5	4	5	5	5	4	5	4	5	4	3	5	4	7	4	5	4
36	4	6	4	4	4	4	5	4	6	3	3	3	5	4	5	4	5	3	5	4	6	3	4	5
37	6	5	3	5	4	4	5	4	4	3	4	6	4	4	5	6	5	3	6	5	4	6	4	5
38	5	4	3	6	5	4	5	4	4	5	4	4	5	4	5	6	4	6	5	5	5	4	4	4
39	3	3	5	3	3	4	6	6	4	5	6	5	4	5	4	3	4	4	6	3	4	5	3	4
40	3	4	4	4	5	4	5	5	5	4	3	4	4	5	4	6	3	5	6	6	6	4	4	4
41	3	4	6	3	4	4	3	6	6	6	5	5	4	5	3	5	6	5	5	5	5	6	3	4
42	5	3	5	6	3	4	5	3	6	5	4	6	5	6	4	5	5	6	4	6	4	4	3	5
43	4	4	7	4	5	5	5	4	4	4	6	5	5	4	3	5	6	4	5	5	4	4	4	4
44	6	4	4	4	4	4	4	5	5	3	4	5	5	5	5	3	6	3	5	5	3	5	5	4
45	5	4	4	4	6	5	5	5	5	3	4	5	5	4	4	5	5	6	3	5	4	4	4	4
46	3	6	6	4	4	3	4	4	4	5	5	6	4	5	3	4	4	5	5	5	4	4	4	6
47	5	5	4	4	6	4	5	3	3	5	4	4	4	5	8	4	4	4	4	5	4	8	4	5
48	5	4	3	5	3	6	5	5	6	4	6	4	4	5	3	5	5	3	3	5	4	4	3	4
49	5	5	6	4	6	6	4	4	4	4	4	4	5	4	5	4	4	5	3	5	5	4	4	5
50	6	5	5	6	5	3	7	4	4	3	3	4	5	4	3	6	4	4	6	5	6	4	5	5
51	5	4	4	5	4	4	4	4	5	4	5	6	4	4	3	6	5	4	6	3	4	4	5	5
52	4	5	5	5	5	5	4	4	6	3	3	6	4	5	5	3	4	6	5	4	4	3	6	3
53	6	5	3	3	4	5	5	3	4	5	4	5	4	6	4	4	5	5	4	6	3	4	4	4
54	5	5	5	5	4	5	4	5	8	4	4	4	4	4	4	5	3	3	4	3	4	6	5	4

buses; 14) the expected objective function of the optimization process of the distribution system in the real-time horizon (second stage optimization objective function of the second level problem).

The optimal day-ahead operational scheduling of distribution system constraints consists of the following terms.

A. Electric power balance constraints

The electric power balance constraint for each bus of the distribution system can be written as (15):

$$P_{DS}^{IPG} + P_{DS}^{DG} \pm P_{DS}^{ESS} \pm P_{DS}^{PLOT} \pm P_{SH}^{Load} - P_{Custom}^{Load} - P_{DS}^{Loss} + P_{DS}^{IMPORT} = 0 \tag{15}$$

The (15) terms are the active power of intermittent power generations, distributed generations, electrical energy systems, parking lots, smart home energy partners, custom loads, electric loss, and imports from the upward electricity market for each simulation interval. It is assumed that all of the custom loads are non-dispatchable loads.

Further, the imported active power from the upward electricity markets constraint can be written as (16):

$$P_{DS\,Min}^{IMPORT} \leq P_{DS}^{IMPORT} \leq P_{DS\,Max}^{IMPORT} \tag{16}$$

The load flow, wind turbines, and photovoltaic arrays constraints that are considered in the optimization process are available in [45].

The upper and lower capacity of electricity generation constraints and the constraints of distributed generation ramp rates are considered in the optimization process [45]. Further, the electrical energy storage and PHEV parking lots' minimum and maximum limits of charge constraints, their charge and discharge constraints, and the maximum charge limits are also considered in the optimization procedure and are not presented for the sack of space [45].

A resiliency index is utilized to assess the resiliency level of the system in the worst-case condition and for the area where the external shock occurs. The resiliency index is defined as (17):
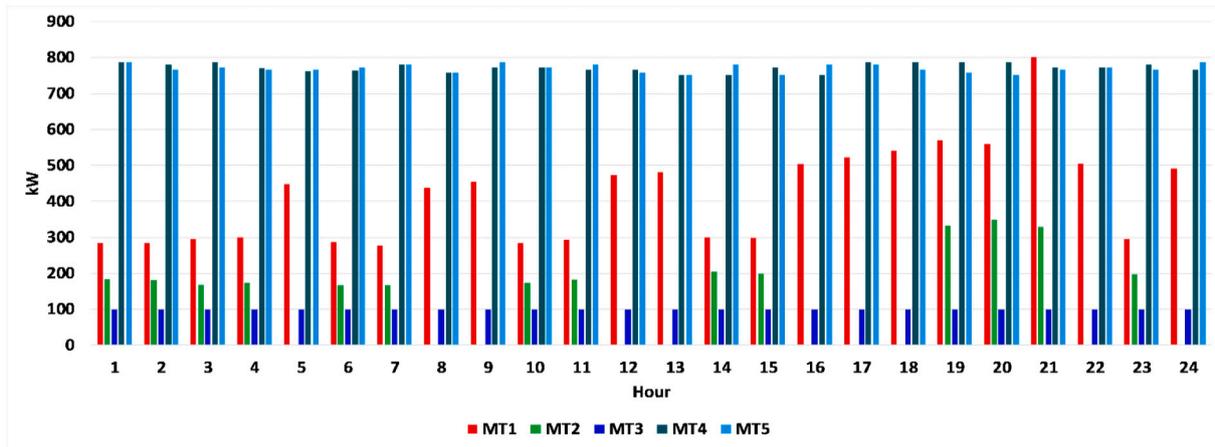
Fig. 22. The optimal electricity generation of microturbines for the most credible external shock.
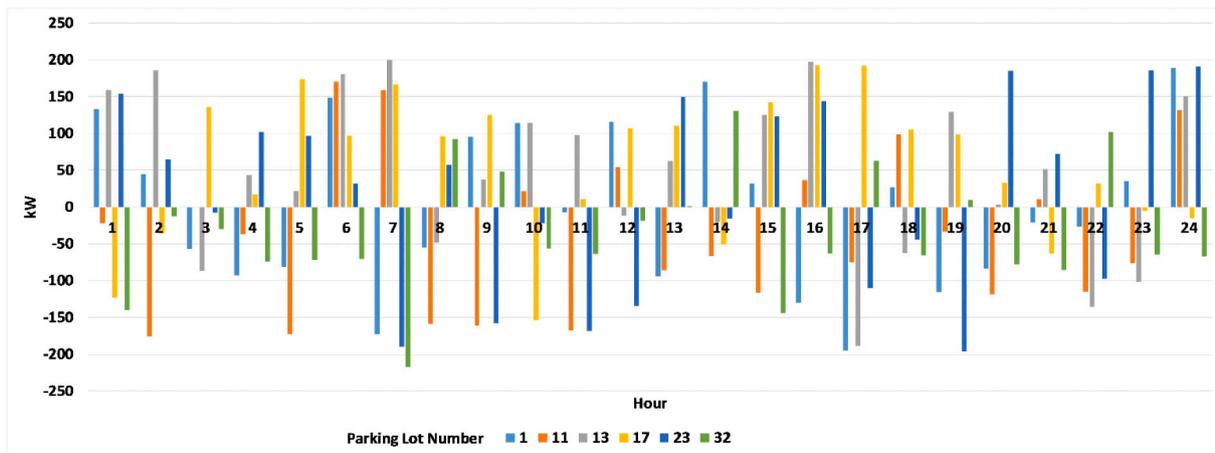
Fig. 23. The estimated values of day-ahead electricity transactions of PHEV parking lots for one of the most credible external shock conditions.

$$RI = \frac{\sum Served\ Loads\ in\ Contingent\ Conditions}{\sum Served\ Loads\ in\ Normal\ Conditions - \sum Served\ Loads\ in\ Contingent\ Conditions} \tag{17}$$

The resiliency index tends to the infinite for these conditions:

1) In the areas where external shocks have not occurred,
2) The area where the external shock has occurred and there are adequate distributed energy resources to recover from contingent conditions.

Further, a day-ahead arbitrage index is defined that detects the expected benefits of arbitrage opportunities of smart homes in the day-ahead market (18):

$$ARI^{DA} = \left(\mathbb{Z}^{DA}_{DS|No\ AR} - \mathbb{Z}^{DA}_{DS} \right) / \mathbb{Z}^{DA}_{DS|No\ AR} \tag{18}$$

$\mathbb{Z}^{DA}_{DS|No\ AR}$ and $\mathbb{Z}^{DA}_{DS}$ are the objective functions of (14) without and with arbitrage opportunities. Higher values of ARI^{DA} present the reduced surplus and resiliency of the distribution system based on the arbitrage process of smart homes.

2.7. Optimal operation of distribution system in real-time normal conditions (second stage of second level problem)

The distribution system operator optimizes its system's control variables every 15 min for real-time operational scheduling of the system. The DSO control variables for the real-time normal operational conditions can be categorized into the following groups:

- The real-time dispatching of the system distributed energy resources, dispatchable and deferrable loads of saver mode of smart homes, and energy partner mode of smart homes distributed energy resources,
- Penalizing smart homes that utilize arbitrage strategy for the real-time horizon,
- Changing the direct load control fees for the real-time horizon.

The objective functions of the second stage of the second level problem are the maximization of distribution system profit in the real-time horizon, which can be written as (19):
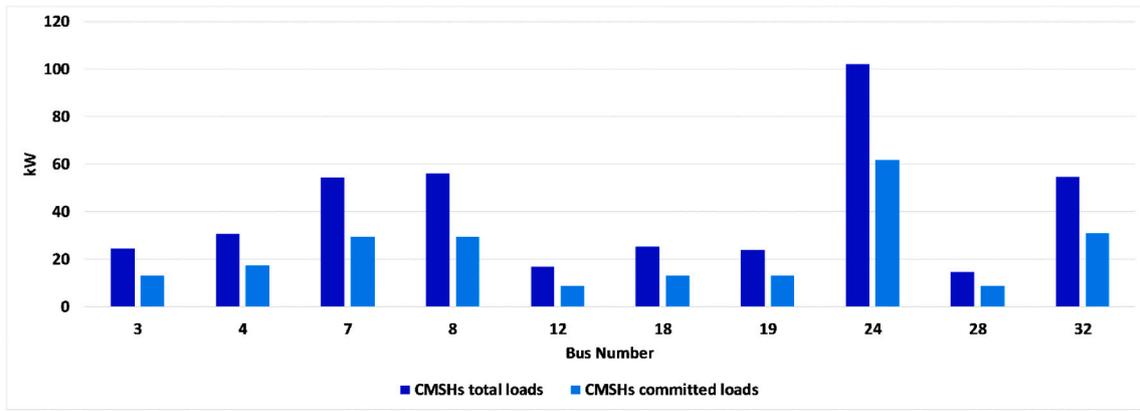
(a)
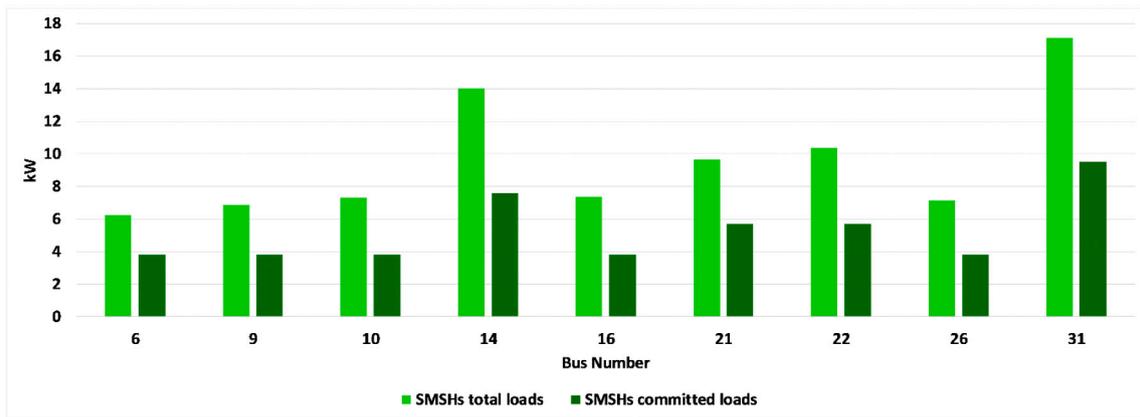
(b)

Fig. 24. (a) The value of load commitment of CMSHs for the most credible external shock, (b) the value of load commitment of SMSHs for the most credible external shock.

Table 6
The sensitivity analysis of the 33-bus test system.

	A1	A2	A3	A4	A5	A6	A7	A8	A9
Case 1	18.67	6	5	145009.6	6369.45	7389.937	5357.063	0.20129	5.526200
Case 2	30	6	5	139821.3	6291.64	7298.319	5277.629	0.23921	4.326914
Case 3	50	6	5	135923.6	6019.21	7102.391	5156.394	0.22362	4.321262
Case 4	30	20	5	128921.2	5893.14	6892.72	4987.961	0.25693	4.120903
Case 5	30	20	20	109281.1	5625.78	6514.28	4723.412	0.26951	3.921481
Case 6	50	20	20	111987.2	5729.31	6715.96	4789.175	0.23512	4.292192

A1: EPSHs Percent, A2: SMSHs Percent, A3: CMSHs Percent, A4: expected average daily operational and energy not supplied costs (MUs), A5: average daily locational marginal (MUs), A6: maximum daily locational marginal (MUs), A7: minimum daily locational marginal (MUs), A8: average daily arbitrage index, A9: expected average number of switching to recover the system.

$$Max\ \mathbb{Z}_{DS}^{RT} = \sum_{k=1}^{k+1} \begin{pmatrix} W_5 \cdot \left(- C_{DS}^{IPG\ RT} - C_{DS}^{DG\ RT} - C_{DS}^{ESS\ RT} - C_{DS}^{PLOT\ RT} - \\ C_{DS}^{Purchase\ RT} - \sum_{NSL} CIC + B_{DS}^{Sell\ RT} - C_{DS}^{DRP\ RT} - C_{DS}^{AR\ RT} \\ + \sum Penalty^{active\ RT} + \sum Penalty^{reactive\ RT} \right) + W_6 \cdot RI - W_7 \cdot \sum_{NB} LMP \end{pmatrix}$$

(19)
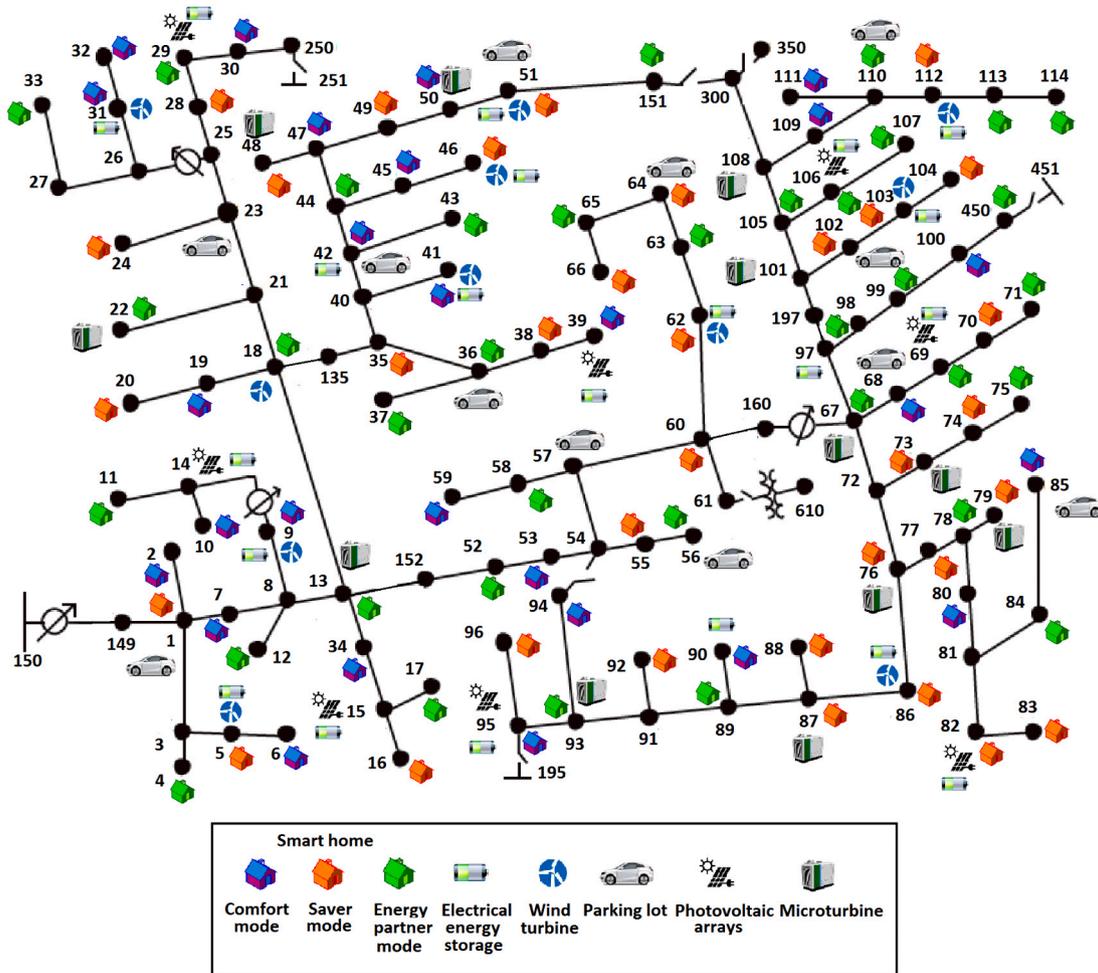
Fig. 25. The modified 123-bus IEEE test system.
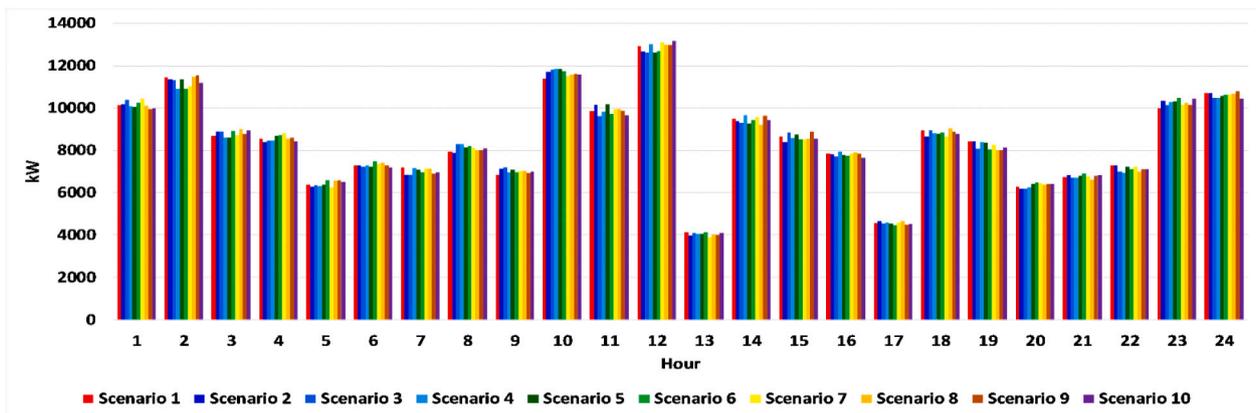
Fig. 26. The day-ahead forecasted electrical load for different scenarios.

The objective function is divided into thirteen terms: 1) the cost of distribution system intermittent power generation ($C_{DS}^{IPG\ RT}$); 2) the cost of distribution system distributed generation ($C_{DS}^{DG\ RT}$); 3) the cost of distribution system energy storage system ($C_{DS}^{ESS\ RT}$); 4) the cost of distribution system PHEV parking lots ($C_{DS}^{PLOT\ RT}$); 5) the distribution system energy cost purchased from the upward market ($C_{DS}^{Purchase\ RT}$); 6) the energy not supplied costs (*ENSC*); 7) the benefit of energy sold to the smart homes ($B_{DS}^{Sell\ RT}$); 8) the cost of demand response programs (C_{DS}^{DRP} ^{RT}); 9) the cost of energy and ancillary services arbitrage imposed by smart homes ($C_{DS}^{AR\ RT}$); 10) the benefit of smart homes active power mismatch penalties ($\sum Penalty^{active\ RT}$); 11) the benefit of smart homes reactive power mismatch penalties ($\sum Penalty^{reactive\ RT}$); 12) the resiliency index; 13) the sum of the locational marginal price of system buses.

The constraints of the second stage objective function consist of the day-ahead optimization process of the distribution system.

The real-time arbitrage index detects the expected benefits of arbi-
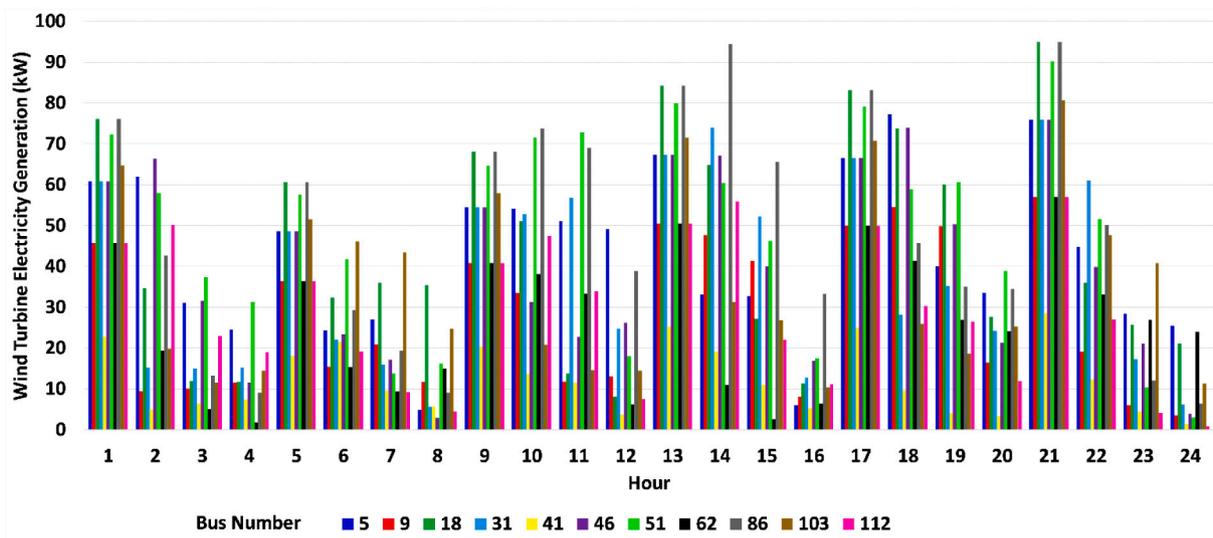
Fig. 27. The forecasted photovoltaic electricity generation for different scenarios.
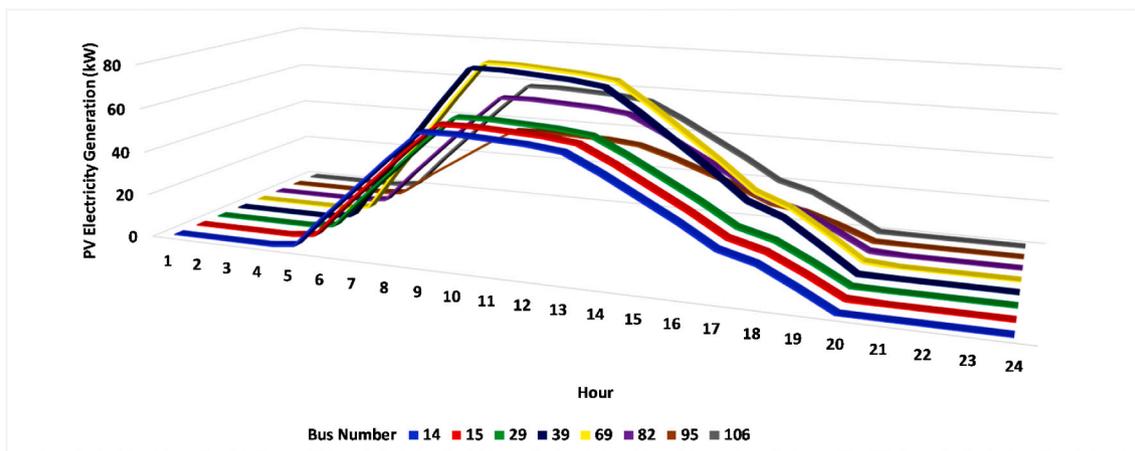
Fig. 28. The forecasted photovoltaic electricity generation for different scenarios.
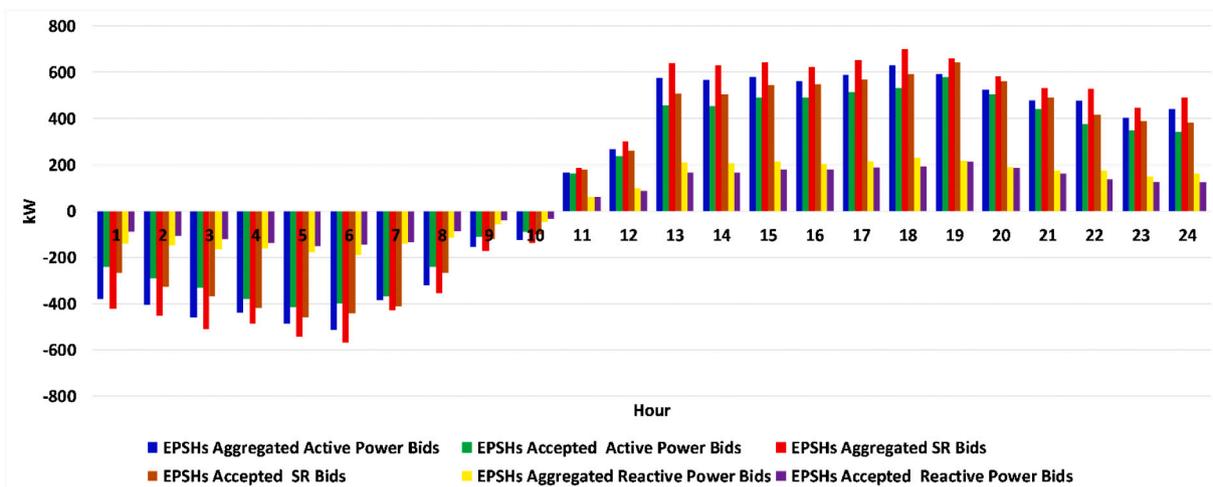
Fig. 29. The day-ahead aggregated active power bidding and their accepted values of energy partner mode of smart homes for one of the reduced scenarios.
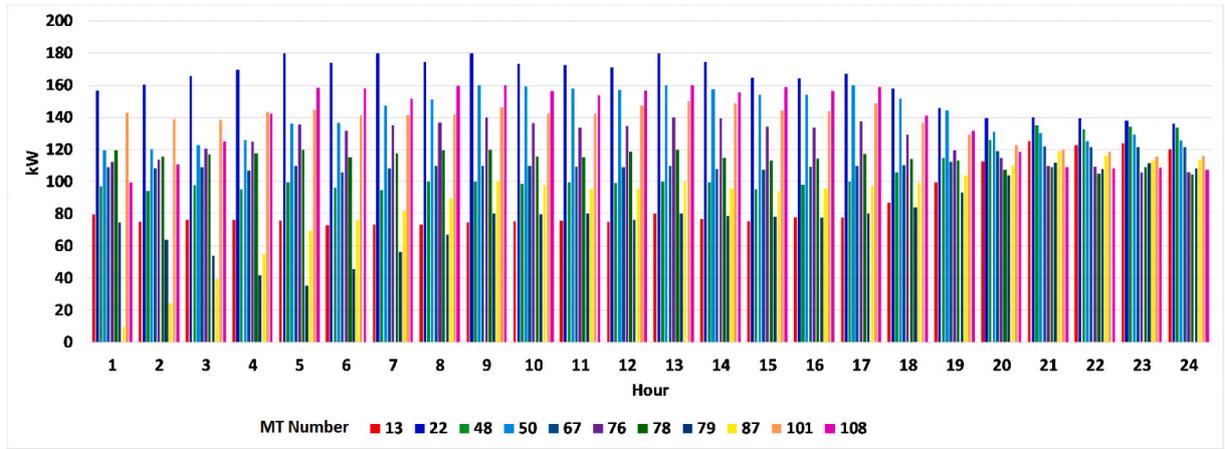
Fig. 30. The estimated values of day-ahead active generations of microturbines for one of the reduced scenarios.
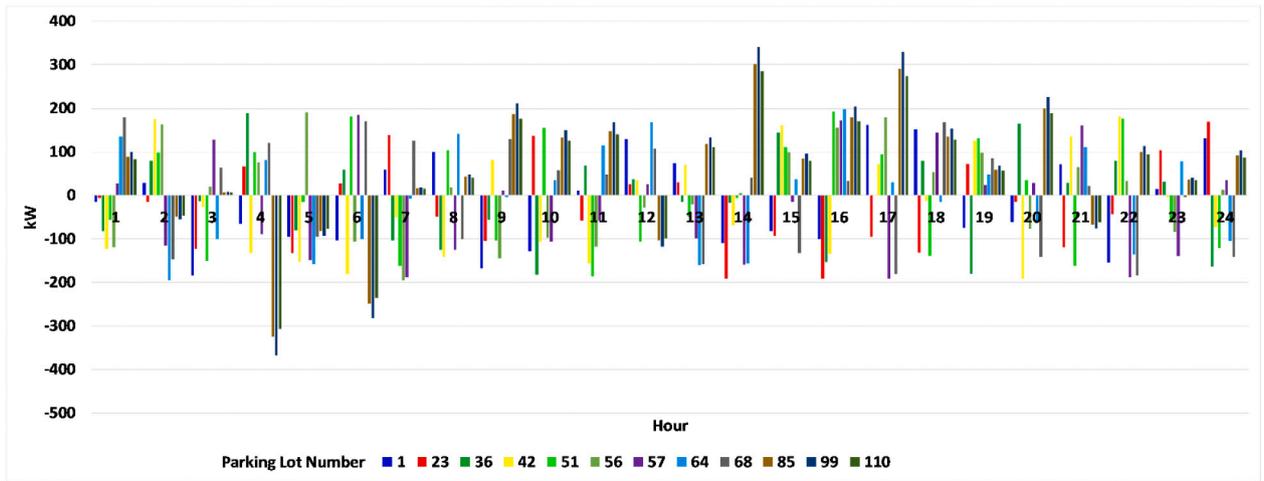
Fig. 31. The estimated values of day-ahead electricity transactions of PHEV parking lots for one of the reduced scenarios.

trage opportunities of smart homes in the real-time market and this index is defined as (20):

$$ARI^{RT} = \left(\mathbb{Z}^{RT}_{DS|No\ AR} - \mathbb{Z}^{RT}_{DS} \right) \Big/ \mathbb{Z}^{RT}_{DS|No\ AR} \tag{20}$$

$\mathbb{Z}^{RT}_{DS|No\ AR}$ and $\mathbb{Z}^{RT}_{DS}$ are the objective functions of (19) without and with arbitrage opportunities. Same as the day-ahead index of the arbitrage index, higher values of ARI^{RT} present the reduced surplus and resiliency of the distribution system for the real-time horizon based on the arbitrage process of smart homes.

2.8. Optimal operation of distribution system in external shock conditions (third stage of second level problem)

The distribution system operator updates its data and detects any external shock impacts. The distribution system sectionalizes its system into multi-microgrids to reduce the impacts of external shocks. Thus, the system control variables for external shock conditions can be categorized into the following groups:

$$Min\ \mathbb{S}^{ESC}_{DS} = \sum_{NST} \sum_{k=1}^{k+1} \begin{pmatrix} W_8 \cdot \left(C^{IPG\ RT}_{DS} + C^{DG\ RT}_{DS} + C^{ESS\ RT}_{DS} + C^{PLOT\ RT}_{DS} + C^{Purchase\ RT}_{DS} - B^{Sell\ RT}_{DS} \right) \\ + C^{DRP\ RT}_{DS} + C^{AR\ RT}_{DS} - \sum Penalty^{active\ RT} - \sum Penalty^{reactive\ RT} \Big) \\ + W_9 \cdot \sum_{NSL} CIC - W_{10} \cdot RI + W_{11} \cdot \sum_{NCS} Y + W_{12} \cdot \sum_{NB} LMP \end{pmatrix} \tag{21}$$
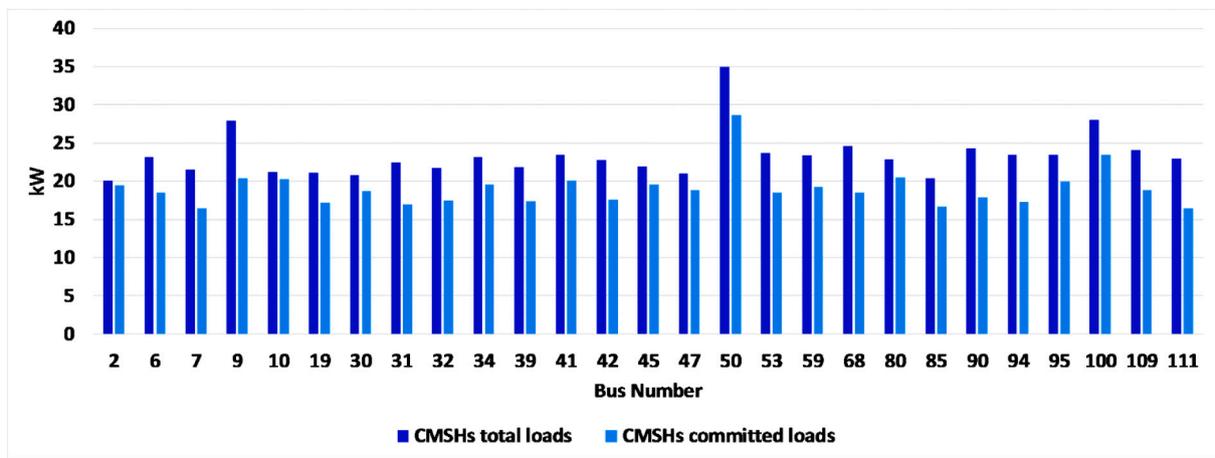
(a)
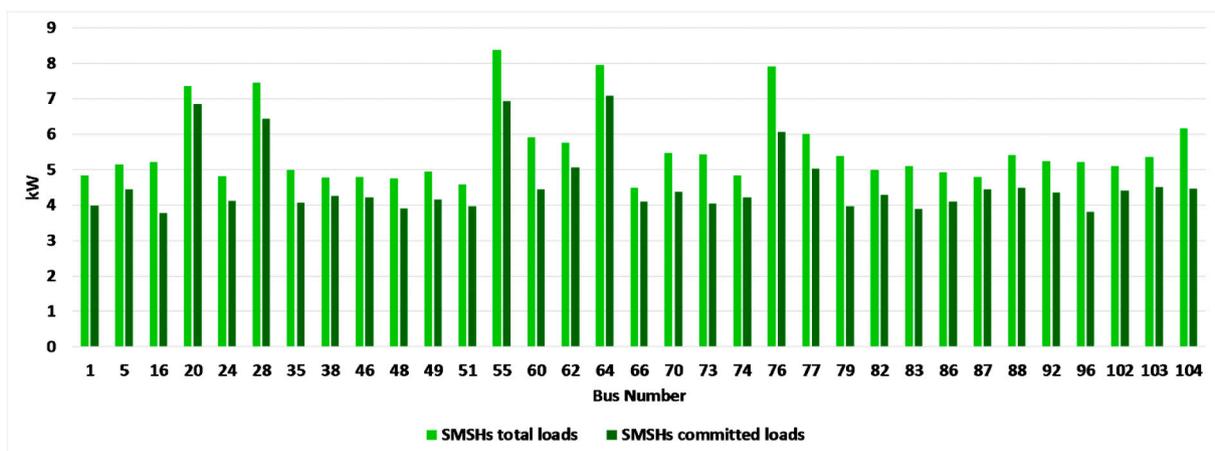
(b)

Fig. 32. (a) The value of load commitment of CMSHs, (b) the value of load commitment of SMSHs.
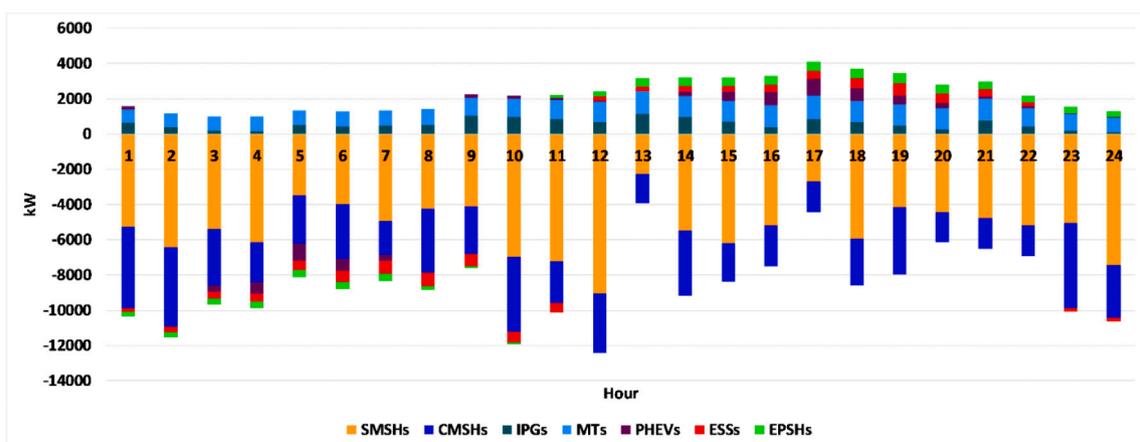
Fig. 33. The distributed energy resources and smart homes electricity transactions for the day ahead optimization interval.

- The real-time dispatching of the system distributed energy resources, dispatchable and deferrable loads of saver mode of smart homes, and energy partner mode of smart homes distributed energy resources,
- Load curtailment of all types of smart homes,
- Sectionalizing the distribution system into multi-microgrids.

The objective functions of the external shock condition of the distribution system can be written as (21):

The objective function is divided into fourteen terms: 1) the cost of distribution system intermittent power generation ($C_{DS}^{IPG\ RT}$); 2) the cost
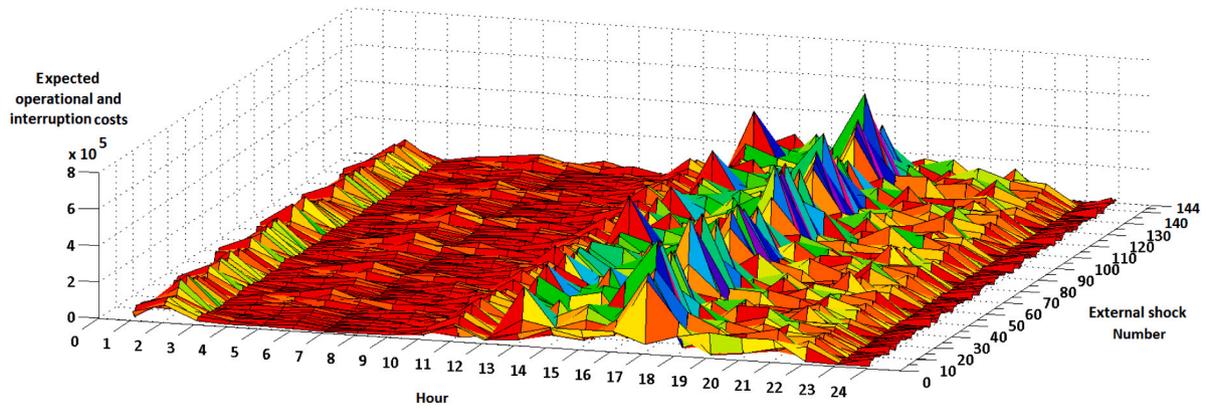
Fig. 34. The aggregated expected operational and energy not supplied costs for the 144 most credible external shock and day-ahead optimization horizon.
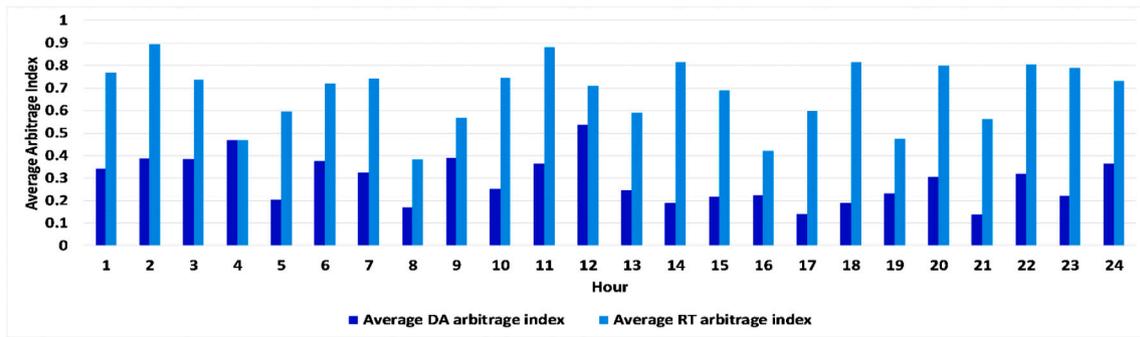
Fig. 35. The estimated values of arbitrage index for the 144 most credible external shocks and day-ahead optimization horizon.
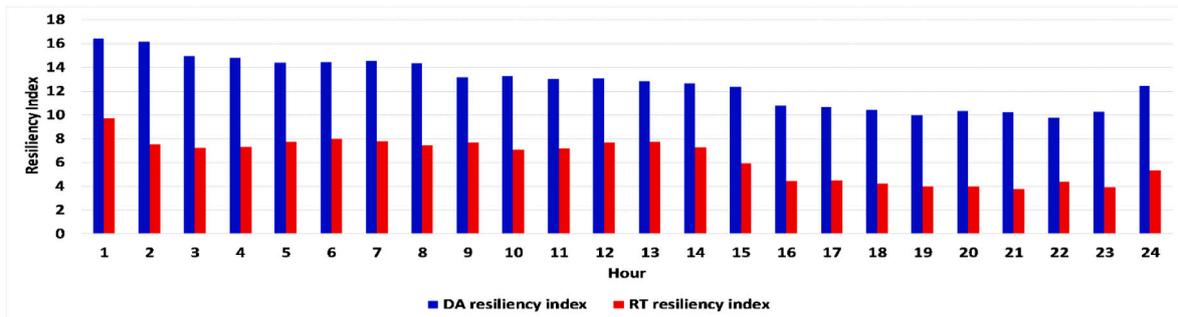
Fig. 36. The estimated values of resiliency index for day-ahead and real-time optimization horizons without implementing the proposed method.

of distribution system distributed generation ($C_{DS}^{DG\ RT}$); 3) the cost of distribution system energy storage system ($C_{DS}^{ESS\ RT}$); 4) the cost of distribution system PHEV parking lots ($C_{DS}^{PLOT\ RT}$); 5) the distribution system energy cost purchased from the upward market ($C_{DS}^{Purchase\ RT}$); 6) the benefit of energy sold to the smart homes ($B_{DS}^{Sell\ RT}$); 7) the cost of demand response programs ($C_{DS}^{DRP\ RT}$); 8) the cost of energy and ancillary services arbitrage imposed by smart homes ($C_{DS}^{AR\ RT}$); 9) the benefit of smart homes active power mismatch penalties ($\sum Penalty^{active\ RT}$);10) the benefit of smart homes reactive power mismatch penalties ($\sum Penalty^{reactive\ RT}$); 11) the interruption cost of comfort mode customers; 12) the resiliency index; 13) the boundary lines of multi-microgrids that the zero value of X means the electricity flow in the boundary line equals zero; 14) the sum of the locational marginal price of system buses.

The thirteen term of (21) determines the boundary lines of microgrids and the zero value of Y means the electricity flow in the boundary line equals zero. The boundary lines are equipped with normally closed switches that can be opened in contingent conditions to change the

topology of the distribution system into multi-microgrids.

The constraints of the optimal operation of the distribution system in external shock conditions are the same as the real-time optimization process and are not presented for the sack of space.

3. Optimization algorithm

The first and second-level optimization models are linear programming and mixed integer nonlinear programming problems, respectively. The following solvers are utilized to solve the problems:

1. The first and second stages of the first level problem are solved by the CPLEX solver of GAMS,
2. The first and second stages of the second-level problem are solved by the DICOPT solver of GAMS,
3. The third stage of the second-level problem is solved by the SCIP solver of GAMS.
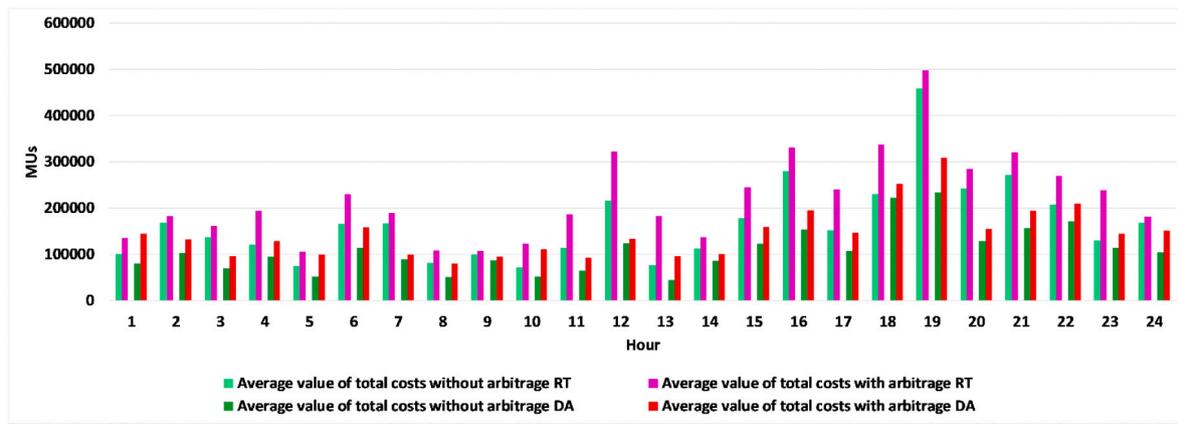
Fig. 37. The estimated values of operational costs of the system for the day-ahead and real-time optimization horizons with and without the arbitrage mechanism of smart homes.
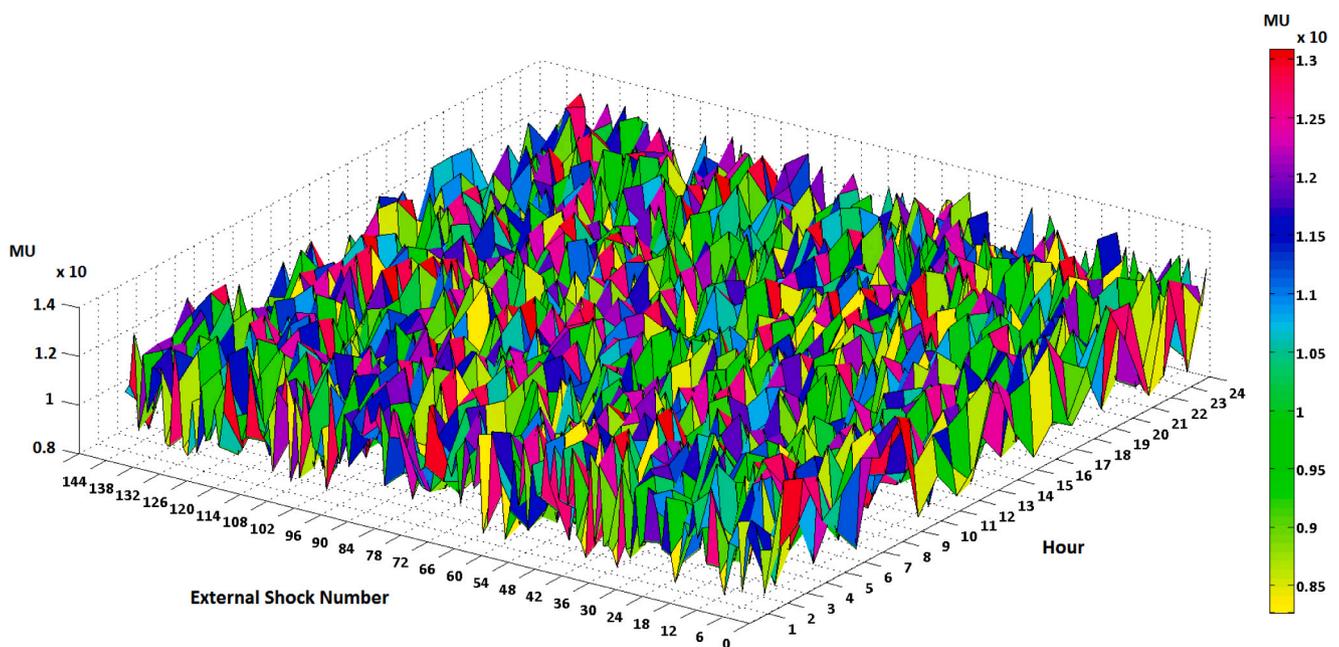
Fig. 38. The estimated values of the highest value of locational marginal of the system for external shocks considering the arbitrage process of smart homes.

Fig. 2 depicts the flowchart of the proposed algorithm. As shown in Fig. 2, the proposed optimization algorithm is decomposed into optimal operational scheduling of smart homes and distribution system in the first and second levels, respectively. The first level problem is decomposed into optimal operational scheduling of smart homes in the day-ahead (first stage) and real-time (second stage) optimization horizons, respectively. The second level problem consists of three stages of optimization problems for optimal operation of the distribution system in normal and contingent conditions. At the first stage of the second level problem, the distribution system dispatches its distributed energy resources for the day-ahead market in normal conditions. At the second stage of the second-level problem, the system schedules the system's resources for the real-time horizon. Finally, in the third stage of the second-level problem, the impacts of external shocks on the distribution system are analyzed, system resources are redispatched, and the topology of the system is optimized.

4. Simulation results

4.1. Simulation results for 33-bus system

The proposed method was assessed by 33-bus and 123-bus IEEE test systems. Fig. 3 depicts the topology of the 33-bus test system [45]. Table 2 presents the characteristics of distributed energy resources.

Table 3 shows the operational costs and capacity of microturbines. The scenario generation and reduction scenarios are presented in Table 4.

Figs. 4, 5, and 6 present the day-ahead forecasted load, per unit values of electricity generation of photovoltaic arrays, and per unit values of wind turbines for one of the reduced scenarios, respectively. Fig. 7 presents the forecasted day-ahead electricity and ancillary services prices for one of the reduced scenarios. The MU stands for the monetary unit.

Table 7
The number of switching of system switches to restore the system from external shock impacts.

Ext. Shock	1	2	3	4	5	6	7	8	9	10	11	12	13	14	15	16	17	18	19	20	21	22	23	24	25	26	27	28	29	30	31	32	33	34	35	36
1	6	4	6	4	4	4	6	5	4	6	4	6	5	4	3	5	3	3	4	6	4	5	3	6	5	4	4	3	4	6	4	3	5	6	6	6
2	4	5	5	6	5	5	5	5	5	5	3	4	5	5	4	4	4	5	4	4	6	4	4	4	3	4	5	4	5	5	4	4	3	5	6	6
3	5	4	5	3	6	3	5	4	5	4	5	4	5	4	4	4	4	5	3	3	5	4	4	5	4	5	5	6	4	6	6	5	5	4	3	3
4	4	3	6	5	3	6	5	3	3	3	4	6	5	4	4	5	3	5	3	5	5	6	5	5	6	4	4	4	3	5	4	5	4	5	4	6
5	3	4	5	4	3	4	4	5	4	6	6	6	3	5	5	4	5	4	6	6	5	3	6	3	8	4	6	5	3	6	6	4	5	5	5	5
6	3	4	3	4	6	4	4	4	5	6	5	6	5	4	5	5	5	5	6	6	4	6	3	4	4	3	6	4	5	5	3	4	4	4	4	3
7	5	4	5	4	4	6	3	5	5	4	6	5	5	3	4	5	3	4	5	3	6	3	4	6	6	3	5	6	4	3	4	4	3	3	6	4
8	5	5	5	4	4	4	4	6	5	3	4	5	4	6	5	4	4	6	6	6	3	4	6	5	4	5	5	5	4	3	5	5	5	3	6	6
9	4	5	4	5	6	4	5	4	5	4	4	5	5	5	5	6	5	5	3	5	4	5	4	3	4	4	3	6	5	8	4	4	6	3	6	6
10	6	4	4	6	5	3	4	5	4	4	7	5	4	6	6	4	5	4	6	3	5	5	5	4	6	4	5	5	4	4	5	6	5	3	5	3
11	5	4	4	4	6	5	5	6	4	4	4	5	4	6	5	4	6	5	4	5	4	4	3	5	3	4	4	3	5	5	5	4	5	4	3	5
12	5	6	4	5	4	3	4	6	5	5	3	6	5	5	4	3	3	5	4	5	3	4	5	5	5	7	4	3	3	3	4	4	5	6	6	5
13	6	6	4	5	3	3	4	3	4	6	5	4	5	3	6	5	4	6	6	5	5	3	3	3	5	6	4	3	5	4	5	3	3	5	4	4
14	3	4	3	5	4	5	5	5	4	5	6	5	4	6	5	4	5	3	6	6	3	5	4	4	3	3	5	4	6	5	5	3	3	4	3	3
15	4	5	4	4	4	6	4	4	4	4	5	4	6	5	4	5	4	4	4	5	3	5	4	4	5	5	3	4	3	5	4	4	4	4	4	4
16	4	5	4	6	5	4	6	3	3	5	5	5	3	6	6	4	5	5	5	6	6	3	6	6	6	5	4	8	4	5	4	6	4	3	4	3
17	5	6	4	6	6	5	4	6	5	4	5	3	4	4	4	5	3	4	6	4	4	5	4	3	6	5	5	3	4	4	5	5	5	4	5	4
18	3	6	5	5	4	6	4	5	5	5	6	4	4	5	5	6	4	5	6	4	6	5	6	6	5	3	3	4	3	5	5	4	4	5	3	4
19	5	4	5	4	4	4	6	3	6	5	8	5	4	3	5	5	3	5	3	4	3	3	5	4	5	4	4	5	5	5	6	4	4	4	3	4
20	3	3	5	5	6	6	4	6	5	5	4	4	3	6	5	5	6	5	6	4	4	6	5	4	5	6	5	3	3	5	4	3	4	4	6	6
21	5	5	5	3	4	6	6	3	5	4	4	4	5	4	5	4	5	5	5	6	5	5	4	4	5	9	5	4	4	3	6	6	5	6	4	4
22	5	3	5	5	5	4	5	3	4	4	4	4	5	3	3	6	5	3	3	4	5	3	5	5	5	5	6	4	3	4	5	6	5	5	5	4
23	4	3	6	5	6	5	3	6	5	4	5	3	8	5	4	3	3	5	3	5	4	3	4	3	4	4	7	5	5	6	6	5	3	4	4	4
24	5	4	5	5	5	5	5	5	6	5	4	6	4	4	6	4	4	5	4	6	5	3	4	4	3	5	4	6	5	4	6	5	4	6	4	4

Ext. Shock	37	38	39	40	41	42	43	44	45	46	47	48	49	50	51	52	53	54	55	56	57	58	59	60	61	62	63	64	65	66	67	68	69	70	71	72
1	4	5	6	4	5	4	6	4	4	5	4	6	3	5	5	5	4	3	3	5	4	3	4	3	3	4	4	6	3	5	4	6	5	3	4	4
2	3	4	5	4	3	3	4	5	4	5	4	5	4	5	6	5	5	6	5	3	4	6	4	5	3	4	6	5	3	6	4	6	3	4	4	3
3	5	6	6	3	3	6	5	4	3	4	4	3	4	4	3	4	4	6	3	3	4	5	4	3	4	5	5	5	5	4	4	4	6	3	3	6
4	3	5	3	4	4	5	4	5	5	3	5	3	4	5	4	5	6	4	6	5	5	5	5	4	5	4	5	5	4	4	3	4	4	6	5	5
5	5	6	5	3	3	4	5	3	4	5	5	5	8	6	4	5	7	4	6	4	5	6	4	5	3	5	4	4	5	5	5	5	5	5	5	5
6	4	5	3	5	6	5	4	5	6	3	4	4	4	5	4	6	5	4	3	5	5	6	6	5	3	4	4	5	6	5	5	3	5	5		5
7	4	6	5	4	5	6	4	4	3	4	3	5	4	5	5	4	5	4	4	5	6	6	5	5	6	3	5	4	5	3	5	5	5	5		5
8	5	4	5	4	4	4	5	3	5	3	4	4	3	4	4	4	5	3	9	4	6	4	4	3	5	3	3	5	6	4	4	4	6	4	6	6
9	4	5	3	5	4	5	5	4	3	4	4	3	3	3	3	6	6	4	3	3	3	4	6	5	6	5	5	6	4	5	4	4	4	3	4	6
10	3	4	5	6	4	4	3	5	5	5	3	5	6	5	6	4	4	5	5	3	4	5	4	3	3	4	5	5	5	6	4	5	5	5	5	5
11	5	5	4	4	4	6	4	6	5	6	4	6	4	6	6	5	3	5	5	6	5	3	3	5	6	3	5	5	4	4	5	4	4	3	4	3
12	3	6	6	5	5	5	5	6	5	4	6	3	5	3	4	6	6	4	5	4	5	6	6	5	3	6	5	5	6	5	5	5	5	5	6	4
13	6	5	4	4	4	4	6	5	3	5	4	5	4	4	4	5	4	6	6	5	5	5	4	4	4	6	3	8	5	3	5	3	6		—	
14	5	4	3	4	6	4	3	6	6	4	5	5	5	5	5	4	4	5	8	5	5	4	3	4	3	5	4	5	4	5	5	4	5	5		
15	6	5	4	6	6	5	4	6	6	5	5	4	3	4	5	5	4	3	5	4	4	5	4	4	4	3	3	5	4	5	4	5	5			
16	5	3	3	6	6	6	6	5	3	5	6	5	3	5	4	4	4	4	5	3	4	5	4	5	5	4	3	3	3	3	5	4	5			
17	5	6	6	5	4	5	4	5	4	4	6	4	4	4	5	3	5	4	3	4	6	4	6	3	3	4	3	4	5	3	5	3	4			
18	5	3	3	4	4	5	5	4	5	4	5	3	6	4	3	5	6	3	4	4	4	4	3	5	4	4	5	5	4	4	4	5	5			
19	5	5	3	3	6	5	4	3	3	5	6	3	4	5	6	3	6	3	5	6	5	5	3	5	5	4	3	5	5	5	5	5	3	4		
20	5	5	3	5	4	6	3	5	4	5	3	5	4	4	6	4	4	6	5	4	7	5	4	4	3	5	6	7	3	5	4	5	5	5	5	3
21	4	5	4	4	3	3	5	6	4	5	4	4	5	3	5	3	3	3	5	4	4	3	4	4	4	3	4	6	4	5	4	5	5			
22	5	4	3	4	5	4	4	5	4	4	5	5	6	6	6	3	4	5	3	6	5	5	5	6	3	4	5	3	5	6	5	5	5	3		
23	6	4	5	5	6	4	4	6	3	4	4	5	4	5	6	5	5	5	6	3	4	4	5	5	3	5	5	4	5	4	6	5	3	4	4	
24	3	5	5	4	4	5	3	3	5	5	3	5	3	4	5	6	5	5	6	3	4	4	5	4	4	4	5	9	4	4	6	4	4	4		

Ext. Shock	73	74	75	76	77	78	79	80	81	82	83	84	85	86	87	88	89	90	91	92	93	94	95	96	97	98	99	100	101	102	103	104	105	106	107	108
1	4	4	5	5	3	4	4	5	4	5	4	3	4	3	3	5	6	3	3	5	3	6	5	6	4	4	4	6	5	4	3	6	4	4	4	4
2	5	4	4	6	5	5	4	6	4	5	4	4	6	4	4	6	5	5	6	6	4	4	4	6	6	4	5	3	4	3	5	3	6	5	5	
3	6	4	5	5	5	4	4	4	3	4	6	5	5	5	5	6	4	3	4	6	5	5	3	4	4	6	5	4	5	4	5	6	6	6	5	
4	3	4	4	5	4	6	4	6	3	5	5	3	6	3	4	3	3	4	6	5	4	6	6	3	5	6	4	3	4	5	4	5	6	5		
5	5	4	3	4	4	5	4	6	3	5	5	4	4	5	4	4	5	4	6	3	5	4	3	4	5	5	5	3	3	4	4	5	5	4	5	6
6	5	4	4	3	5	4	4	5	5	6	3	4	4	4	3	4	3	5	4	5	5	5	6	5	5	4	6	3	5	5	3	5	5	5	5	3
7	6	4	5	5	5	3	4	4	4	4	4	4	5	5	5	4	5	4	3	3	5	3	3	6	6	6	5	5	6	3	4	5	6	4		
8	6	4	6	3	3	3	6	3	4	3	4	5	3	5	3	6	4	4	5	5	6	4	4	4	4	5	6	4	5	4	6	4	4			
9	3	3	5	5	4	5	5	5	5	5	5	5	4	3	5	5	3	4	4	3	5	4	6	3	4	3	6	5	3	5	6	3	4	5		
10	5	4	5	4	4	4	3	5	4	6	5	4	3	5	4	5	4	5	4	6	4	3	6	5	4	6	5	4	5	6	3	5	5	3		
11	5	5	5	5	6	5	5	5	3	6	5	3	4	4	4	4	6	3	3	3	6	4	5	4	6	5	5	4	4	4	4	3				
12	5	4	5	5	3	4	4	5	4	5	5	4	4	5	5	4	4	5	3	6	4	4	5	5	4	4	3	5	5	3	3	5	5	4		
13	6	5	6	5	5	3	4	4	5	6	5	5	6	5	5	5	5	4	4	3	5	5	3	4	4	3	6	4	4	3	5	5	4	5	3	3
14	6	4	4	6	6	5	5	3	4	6	6	5	6	4	4	5	5	4	4	5	6	6	3	4	5	3	4	3	4	4	5	6	4	6	4	
15	6	4	4	5	3	6	5	5	4	5	4	5	3	4	3	4	4	5	3	4	5	5	4	4	4	4	3	4	6	3	5	4	4			
16	3	5	6	6	5	5	4	5	5	5	4	6	5	5	3	4	4	6	5	4	5	4	4	6	4	5	5	6	5	3	5	3				
17	4	5	5	4	6	4	3	6	5	6	5	3	4	4	5	5	3	4	6	3	4	5	4	8	5	5	5	4	3	3	4	5				
18	4	5	5	6	5	4	4	4	4	5	5	5	3	3	4	5	5	4	4	4	5	6	6	4	5	6	4	5	4	6	4	3	4	5		
19	3	5	4	3	5	6	5	6	5	4	4	4	5	4	7	6	3	5	4	3	4	5	4	3	4	5	5	5	6	5	4	6	5	3	4	
20	3	5	5	4	4	6	6	4	3	4	3	3	4	4	3	5	5	3	3	3	5	4	5	5	5	6	5	4	4	3	3	4	4	3		
21	5	5	3	3	4	4	5	3	5	4	3	3	5	5	4	6	4	5	5	4	5	4	3	4	4	3	4	4	5	5	4	5	6	4		
22	5	5	3	5	3	3	4	6	5	3	4	6	5	5	6	3	5	4	5	4	4	5	5	4	4	4	6	3	4							
23	6	3	5	6	4	4	5	4	4	4	3	3	5	4	6	4	4	3	6	5	4	4	5	5	4	8	4	5	4	4						
24	6	4	5	5	4	5	6	5	5	6	5	6	4	5	6	6	4	3	6	3	6	4	4	5	5	4	4	5	5	6	4	5	5	6		

Ext. Shock	109	110	111	112	113	114	115	116	117	118	119	120	121	122	123	124	125	126	127	128	129	130	131	132	133	134	135	136	137	138	139	140	141	142	143	144
1	5	5	4	6	5	6	5	4	4	5	4	4	3	6	5	6	4	3	5	4	5	4	4	4	6	5	5	5	3	5	4	6	5	6	6	6
2	3	4	6	4	5	4	5	6	4	5	6	5	3	5	3	4	5	6	4	5	5	4	3	5	4	3	3	6	4	3	6	5	4			
3	6	6	4	6	4	5	5	5	5	4	6	5	5	6	4	5	5	4	3	6	5	3	5	4	5	3	4	5	3	6	5	6	4	6	6	4
4	4	5	4	5	6	4	4	5	4	6	6	3	5	5	3	4	5	3	4	3	6	4	3	5	5	5	5	3	5	4	3	5	4	5	4	
5	3	4	5	5	5	5	5	5	6	4	5	4	4	3	3	4	3	4	6	5	3	5	4	5	5	5	3	5	5	5	3	5	5	4	6	
6	3	5	3	6	5	3	3	6	3	5	5	6	3	5	4	3	4	5	3	4	6	5	6	4	5	5	6	3	4	5	5	5	5	3	5	
7	6	4	4	5	6	6	3	3	5	4	5	4	6	4	4	4	3	6	4	4	5	9	6	3	4	4	6	4	5	5	6					
8	6	4	3	4	5	5	5	4	5	4	5	4	5	4	3	5	4	5	5	5	6	5	6	3	3	4	6	3	5	5	4					
9	5	6	3	4	4	5	4	6	6	4	5	5	3	4	4	4	5	4	6	6	5	4	5	5	8	5	4	4	6	3	5	5				
10	3	3	6	3	6	3	5	5	5	5	5	5	4	6	3	4	5	3	6	4	5	6	4	5	4	6	3	5	5	5	3					
11	4	5	3	5	6	6	5	6	5	5	5	4	5	5	4	5	6	3	5	5	6	4	5	5	5	6	6	5	4	6	3	4	6			
12	4	6	6	4	4	5	6	3	5	4	3	6	5	5	4	5	5	5	4	5	6	4	5	5	5	4	5	4	4	5	4					
13	3	5	5	4	4	6	6	3	5	6	3	6	5	5	3	4	3	5	5	6	6	6	4	5	4	5	5	3	5	4	4	5				
14	5	5	3	5	6	5	6	4	4	4	6	4	6	4	5	5	4	3	3	6	5	5	4	4	6	7	5	3	5	3	5	5	4	6	5	
15	4	4	4	6	4	3	6	6	5	3	3	5	4	3	6	4	4	3	5	5	4	4	5	4	4	5	4	5	3	4	6	3	5	5	4	
16	4	5	5	4	3	6	6	5	3	3	5	4	3	6	6	7	6	4	3	5	4	5	4	4	4	4	8	4	5	6	4	3	5	4		
17	5	6	5	5	4	5	4	3	5	3	4	6	5	4	6	3	4	4	5	3	4	5	5	3	5	4	4	4	3	4	4	4	5			
18	3	4	6	3	4	4	3	5	5	4	4	3	5	4	2	6	3	5	4	5	5	4	5	4	5	6	4	6	6	5	4	6	4			
19	3	4	5	4	4	3	3	5	5	4	4	5	3	5	3	4	4	3	5	5	5	5	4	5	4	6	5	4	4	5	3	5	5			
20	4	4	4	3	4	6	5	5	6	4	4	4	5	5	4	5	6	4	4	6	5	3	4	4	5	3	4	4	5	5	4	4	5	4		
21	5	4	6	4	4	6	5	3	5	4	3	4	6	4	3	5	4	6	3	5	5	3	5	3	5	3	6	5	4	5	4	5	4	5	3	
22	5	4	4	4	5	5	4	5	5	6	4	5	5	5	5	5	4	5	4	3	3	6	6	4	5	5	4	4	5	4	6	4	3	4	5	4
23	4	5	5	6	4	5	5	4	3	5	4	3	5	6	4	3	4	4	3	4	4	4	7	3	6	5	5	4	3	6	5	5	3	5	4	6
24	6	5	4	4	5	4	3	3	5	5	5	3	5	6	4	5	6	6	4	3	5	5	5	6	6	5	5	4	6	8	5	5	3	6	4	5

Fig. 8 depicts the forecasted load of the system in the real-time horizon that was carried out for 5 min forecasting intervals.

Fig. 9 (a) and Fig. 9 (b) present the average hourly values of forecasted real-time electricity and ancillary services prices for different scenarios.

4.2. Simulation results for 33-bus system

The optimization process was carried out for the normal operation of the 33-bus system. Different values of energy partner mode, comfort mode, and energy saver mode of smart home loads were considered for the simulation process. When the average hourly arbitrage index was greater than 0.1, the selected values of these parameters were considered as initial values. For the 33-bus system, the initial values of energy partner mode, comfort mode, and energy saver mode of smart home loads were 18.67 %, 5 %, and 5 % of the system peak load, respectively. Other selected values will be discussed in the sensitivity analysis. Fig. 10 (a) and Fig. 10 (b) present the day-ahead active power bidding and their accepted values of energy partner mode of smart homes for one of the reduced scenarios. Figs. 11 (a) and Fig. 11 (b) depict the day-ahead reactive power and spinning reserve bidding and their accepted values of energy partner mode of smart homes for one of the reduced scenarios.

Fig. 12 presents the estimated values of day-ahead active generations of microturbines for one of the reduced scenarios. As shown in Fig. 12, microturbines 3, 4, and 5 were fully committed for the day-ahead horizon and microturbines 1 and 2 were partially loaded to track the electrical load of the system.

Fig. 13 shows the estimated values of day-ahead electricity transactions of PHEV parking lots for one of the reduced scenarios and normal operating conditions. As shown in Fig. 13, the maximum and minimum values of PHEV parking lots were 355.23 kW and −562.95 kW, respectively.

Fig. 14 presents the distributed energy resources and smart homes' electricity transactions for one of the reduced scenarios. The maximum value of aggregated active power injection of energy partner mode of smart homes was 204.65 kW for hour 19. The maximum value of aggregated active power withdrawal of energy partner mode of smart homes was 157.06 kW for hour 5. The net transacted energy of energy partner smart homes was 1303.57 kWh with an average value of 54.31 kWh. The aggregated electrical energy consumption of comfort modes and saver modes of smart homes were 14,451.70 kWh and 4607.83 kWh, respectively. The energy consumptions of comfort and energy saver modes of smart homes were 18.68 %, and 6 % of the electrical load of the system, respectively.

Fig. 15 presents the aggregated expected operational and energy not supplied costs for the 54 most credible external shocks and day-ahead optimization horizon. The average value of aggregated expected operational and energy not supplied costs was 21,081.57 MUs. Further, the maximum value of aggregated expected operational and energy not supplied costs was 104,752 MUs for external shock 15 and hour 19.

Fig. 16 presents the estimated values of the average hourly arbitrage index for day-ahead and real-time optimization horizons. The maximum values of arbitrage indices for day-ahead and real-time markets were 0.45678 for hour 12 and 0.74 for hour 10, respectively. As shown in Fig. 16, the average values of the real-time arbitrage index were greater than the average values of the day-ahead arbitrage index based on the fact that in the real-time market, the energy partner smart homes had more opportunities to gain benefits and sell active power and ancillary services concerning the day-head market.

Fig. 17 presents the estimated values of the average hourly resiliency index for the day-ahead and real-time optimization horizons without implementing the proposed method. The resiliency index of the system tended to the infinity with the proposed method. As shown in Fig. 17, the average values of the real-time resiliency index were lower than the average values of the day-ahead resiliency index based on the fact that in the real-time market, the energy partner smart homes had more opportunities to arbitrage concerning the day-head market. This process decreased the available dispatchable distributed generation variables for the system when the proposed method did not carry out.

Fig. 18 presents the estimated values of the average hourly arbitrage index for the 54 most credible external shocks and day-ahead optimization horizon. The maximum value of the average hourly arbitrage index was one for external shock 9 and hour 12. The energy partner smart homes bids reduced the available distributed energy generation by about 65.98 % concerning the base case. Further, the arbitrage opportunity of energy partner smart homes reduced the resiliency index of the system from infinite to 4.85 when the system operator did not consider the proposed method. Fig. 19 depicts the estimated values of operational costs for the day-ahead and real-time optimization horizons with and without the arbitrage process of smart homes. The expected values of aggregated system costs without and with arbitrage in the day-ahead horizon were 496,763 MUs and 750,259 MUs, respectively. The arbitrage of energy partner smart homes increased the expected values of aggregated system costs by about 51.02 % concerning the no-arbitrage case in the day-ahead market. Further, the expected values of aggregated system costs without and with arbitrage in the real-time horizon were 613,800.36 MUs and 995,218.56 MUs, respectively. The arbitrage of energy partner smart homes increased the expected values of aggregated system costs by about 62.14 % concerning the no-arbitrage case in the real-time market. The proposed method reduced the aggregated system costs in the real-time horizon more than the corresponding costs in the day-ahead market.
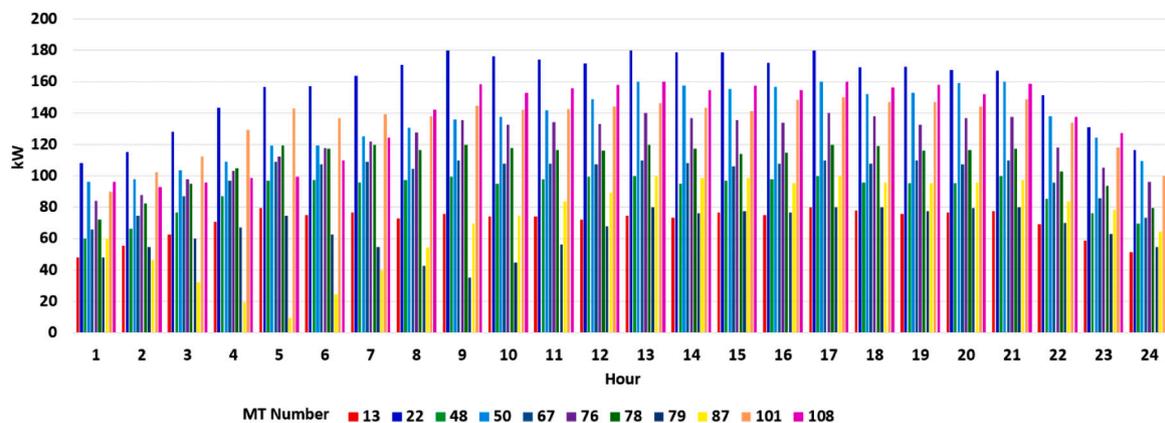

Fig. 39. The optimal electricity generation of microturbines for the most credible external shock.

Fig. 20 (a) and Fig. 20 (b) show the values of load commitment of CMSHs and SMSHs, respectively. As shown in Fig. 20 (a) and Fig. 20 (b), the average values of CMSHs and SMSHs load commitments were 81.97 % and 82.91 %, respectively.

Fig. 21 presents the highest value of locational marginal of the system for external shocks considering the arbitrage process of smart homes. The average value of locational marginal prices was 6.36945 MUs. The maximum value of locational marginal prices was 7.38993 MUs for external shock 40 and hour 2. The minimum value of locational marginal prices was 5.35706 MUs for external shock 13 and hour 17. The average value of locational marginal price was reduced by about 59.38 % concerning the case that the proposed method was not implemented.

Table 5 depicts the number of switching of switches to restore the system from external shock impacts. The optimal restoration of the 33-bus test system required 3–8 switching of the system switches to recover from external shock impacts.

Fig. 22 presents the optimal electricity generation of microturbines for one of the most credible external shocks (external shock number 15 for hour 19 that multiple facilities were out of service between line 2–3 and line 2–19 area and all of the electrical loads of bus 19–22 were impacted by the external shock). When the proposed method was not carried out, the resiliency index of the system decreased to 1.75 and 2.82 for the day-ahead and real-time horizons, respectively. The proposed process recovered the system by multiple switching and the resiliency index of the system tended to the infinity. In this external shock condition, 360 kW of system load was out of service when the proposed method was not implemented.

Fig. 23 depicts the estimated values of day-ahead electricity transactions of PHEV parking lots for the most credible external shock condition. As shown in Fig. 23, the maximum and minimum values of PHEV parking lots were 200.5 kW and −217.38 kW, respectively.

Fig. 24 (a) and Fig. 24 (b) show the values of load commitment of CMSHs and SMSHs for the most credible external shock, respectively. As shown in Fig. 24 (a) and Fig. 24 (b), the average values of CMSHs and SMSHs load commitments were 56.1 % and 55.26 %, respectively.

For sensitivity analysis, five cases were considered. The results are depicted in Table 6 and A1, A2, and A3 parameters were considered as inputs.

As shown in Table 6, for the second and third cases, the expected average daily operational and energy not supplied costs, average daily locational marginal, maximum and minimum values of daily locational marginal, and expected average number of switching to recover system were decreased when the percent of energy partner smart homes was increased. Further, the average daily arbitrage index was increased when the energy partner smart homes percent was increased. For the fourth and fifth cases, the A4-A7 and A9 variables were decreased when the energy partner smart homes percent was increased. Further, the average daily arbitrage index was increased based on the fact that the arbitrage opportunities for energy partners were increased. Finally, for the sixth case, the A4-A7 and A9 variables were increased concerning the fifth case variables. Further, the average daily arbitrage index was decreased based on the fact that the energy partner smart home bidding strategies reduced their profits. It can be concluded that the operational costs of the system were increased when the percentage of energy partner mode of smart homes was increased. Further, the resiliency index reduced when the percentage of energy partner smart homes was increased.

4.3. Simulation results for 123-bus system

The optimization process was performed for the modified 123-bus system. Fig. 25 depicts the topology of the 123-bus test system [46].

Figs. 26, 27, and 28 depict the day-ahead forecasted load, electricity generation of photovoltaic arrays, and wind turbines for different scenarios, respectively.

For the 123-bus system, the initial values of energy partner mode, comfort mode, and energy saver mode of smart home loads were 2 %, 34.67 %, and 63.32 % of system peak load, respectively. Fig. 29 presents the day-ahead aggregated active power bidding and their accepted values of energy partner mode of smart homes for one of the reduced scenarios.

Fig. 30 presents the optimal electricity generation of microturbines for one of the reduced scenarios. Microturbines were not fully loaded and tracked the electrical load. The average value of MT electricity generation was about 94.103 kWh.

Fig. 31 depicts the electricity transaction of PHEV parking lots for one of the reduced scenarios. The maximum and minimum values of PHEV parking lots' electricity transactions were 341.29 kW and −367.93 kW, respectively.

Fig. 32 (a) and Fig. 32 (b) present the values of load commitment of CMSHs and SMSHs, respectively. As shown in Fig. 32 (a) and Fig. 32 (b), the average values of CMSHs and SMSHs load commitments were 81.64 % and 83.1 %, respectively.

Fig. 33 presents the distributed energy resources and smart homes' electricity transactions for the day ahead optimization interval.

The maximum value of aggregated active power injection of energy partner mode of smart homes was 578.7821 kW for hour 19. The
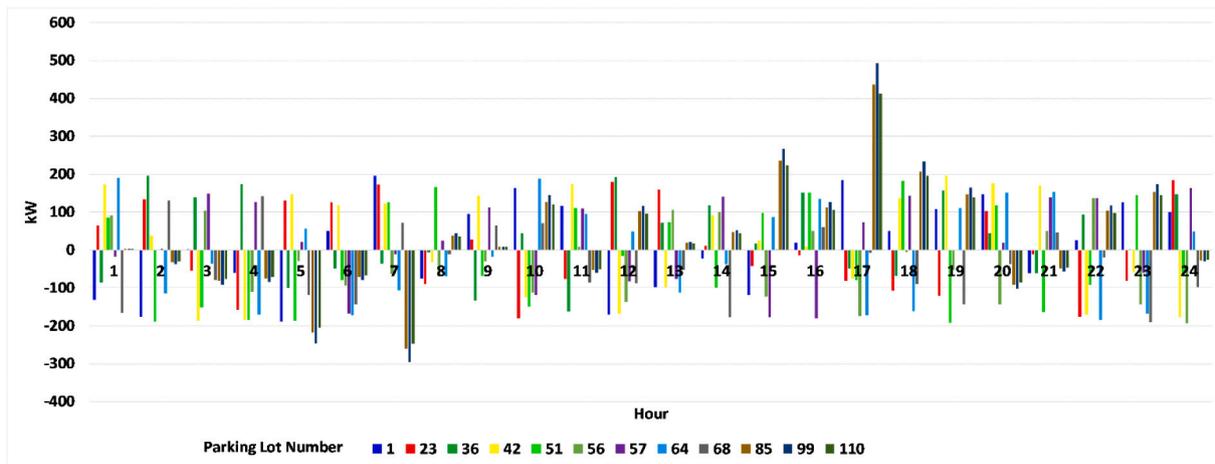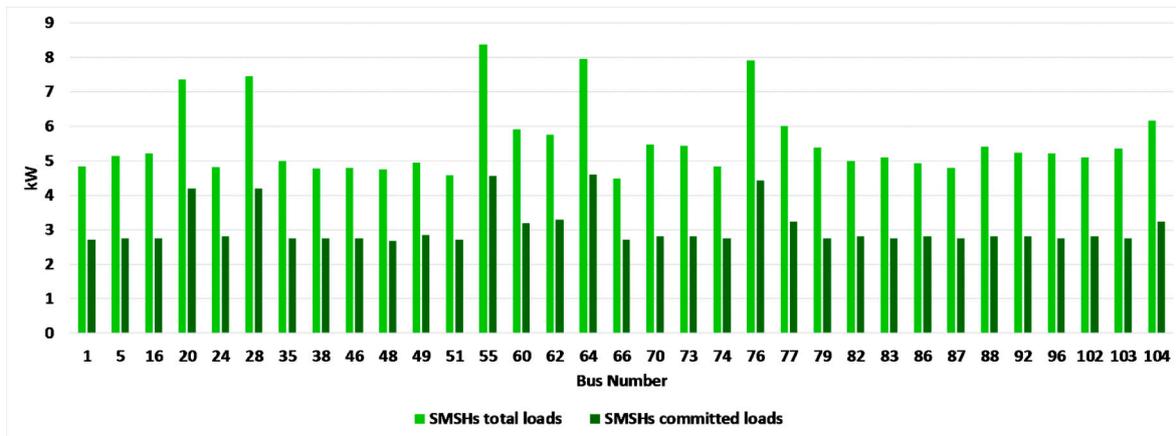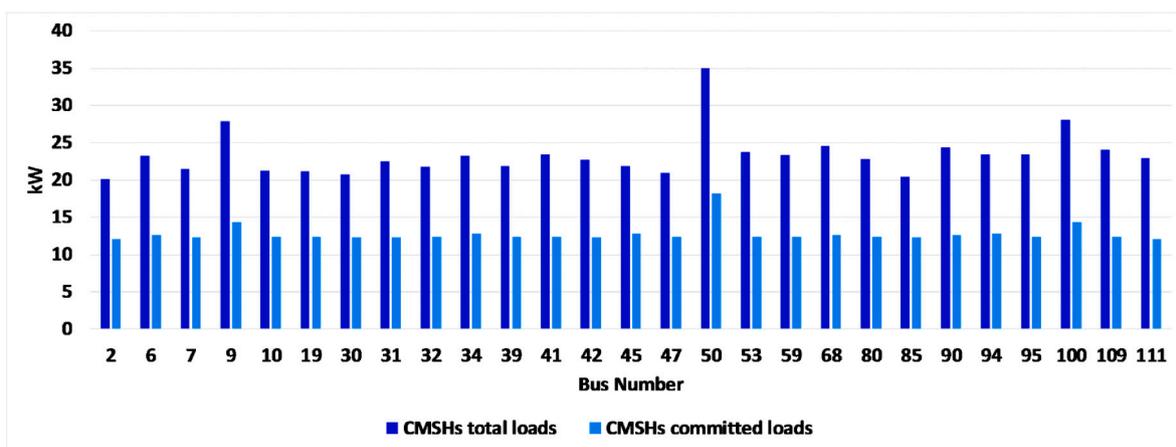

Fig. 40. The estimated values of day-ahead electricity transactions of PHEV parking lots for one of the most credible external shock condition.

(a)

(b)

Fig. 41. (a) The value of load commitment of CMSHs for the most credible external shock, (b) the value of load commitment of SMSHs for the most credible external shock.

maximum value of aggregated active power withdrawal of energy partners was 414.13 kW. The net transacted energy of energy partner smart homes was 3079.62 kWh with an average value of 128.02 kWh. The aggregated electrical energy consumption of comfort modes and saver modes of smart homes were 69,808.08 kWh and 12,897.12 kWh, respectively. Fig. 34 presents the aggregated expected operational and energy not supplied costs for the 144 most credible external shocks and day-ahead optimization horizon.

The average value of aggregated expected operational and energy not supplied costs was 68,596.5 MUs. Further, the maximum value of aggregated expected operational and energy not supplied costs was 633,620.2 MUs that was for external shock 128 and hour 17. Fig. 35 presents the estimated values of the arbitrage index for the 144 most credible external shocks and day-ahead optimization horizon.

The maximum value of the arbitrage index was 0.894434 for hour 2. The average values of the real-time arbitrage index were greater than the average values of the day-ahead arbitrage index based on the fact that in the real-time market, the energy partner smart homes had more opportunities to gain profits.

Fig. 36 presents the estimated values of the resiliency index for the day-ahead and real-time optimization horizons without implementing the proposed method. The resiliency index of the system tended to the infinity with the proposed method.

Fig. 37 presents the estimated values of operational costs of the

system for day-ahead and real-time optimization horizons with and without the arbitrage mechanism of smart homes. The expected values of aggregated system costs in day-ahead horizon without and with arbitrage were 2,625,907 MUs and 3,480,230 MUs, respectively. The arbitrage of energy partner smart homes increased the expected values of aggregated system costs by about 43.95 % concerning the no-arbitrage case in the day-ahead market. Further, the expected values of aggregated system costs without and with arbitrage in the real-time horizon were 4,020,217 MUs and 5,309,059 MUs, respectively. The arbitrage of energy partner smart homes increased the expected values of aggregated system costs by about 32.06 % concerning the no-arbitrage case in the real-time market.

Fig. 38 presents the estimated values of the highest value of locational marginal of the system for external shocks considering the arbitrage process of smart homes. The average value of locational marginal prices was 10.66367 MUs. The maximum value of locational marginal prices was 13.07643 MUs for external shock 38 and hour 18.

The minimum value of locational marginal prices was 8.26344 MUs for external shock 56 and hour 20. The average value of locational marginal price was reduced by about 63.98 % concerning the case that the proposed method was not implemented. Table 7 depicts the number of switching of switches to restore the system from external shock impacts.

Fig. 39 presents the optimal electricity generation of microturbines

Table 8
The sensitivity analysis of the 123-bus test system optimization process.

	A1	A2	A3	A4	A5	A6	A7	A8	A9
Case 1	2	63.32	34.67	68596.5	10663.67	13076.43	8263.44	0.2815	4.5167
Case 2	32	33.32	34.67	71239.21	11923.95	14685.21	9385.39	0.3691	3.2317
Case 3	52	13.32	34.67	75367.98	13045.68	15952.17	10983.15	0.3325	3.1092
Case 4	52	33.32	14.68	78923.83	14612.52	17014.32	12982.23	0.2912	2.9624
Case 5	32	53.32	14.68	68217.23	10121.69	12923.77	8123.71	0.3354	3.1838

A1: EPSHs Percent, A2: SMSHs Percent, A3: CMSHs Percent, A4: expected average daily operational and energy not supplied costs (MUs), A5: average daily locational marginal (MUs), A6: maximum daily locational marginal (MUs), A7: minimum daily locational marginal (MUs), A8: average daily arbitrage index, A9: expected average number of switching to recover the system.

for one of the most credible external shocks (external shock number 128 for hour 17 that multiple facilities were out of service between line 8–13 and line 13–18 area and all of the downward electrical loads were impacted by this external shock). When the proposed method was not carried out, the resiliency index of the system decreased to 7.85 and 3.65 for day-ahead and real-time horizons, respectively. The proposed process recovered the system and the resiliency index of the system tended to the infinity.

Fig. 40 depicts the estimated values of day-ahead electricity transactions of PHEV parking lots for the most credible external shock conditions. As shown in Fig. 40, the maximum and minimum values of PHEV parking lots were 493.51 kW and − 295.8 kW, respectively.

Fig. 41 (a) and Fig. 41 (b) present the values of load commitment of CMSHs and SMSHs for the most credible external shock, respectively.

As shown in Fig. 41, the aggregated energy of CMSH and SMSH loads were 630.59 kWh and 183.52 kWh, respectively. However, the aggregated energy of CMSH and SMSH committed loads were 345.01 kWh and 101.41 kWh, respectively. The optimization process committed the electrical loads of CMSH and SMSH by about 55.62 % and 54.7 % concerning their base values, respectively.

For sensitivity analysis, five cases were considered and their results are depicted in Table 8. As shown in Table 8, for the second and third cases, the expected average daily operational and energy not supplied costs, average daily locational marginal, maximum and minimum values of daily locational marginal, and expected average number of switching to recover system were decreased when the percent of energy partner smart homes was increased. Further, the average daily arbitrage index was increased when the energy partner smart homes percent was increased. For the fourth and fifth cases, the A4-A7 and A9 variables were decreased when the energy partner smart homes percent was increased. Further, the average daily arbitrage index was increased based on the fact that the arbitrage opportunities for energy partners were increased. Finally, for the sixth case, the A4-A7 and A9 variables were increased concerning the fifth case variables when the energy partner smart homes percent was increased. Further, the average daily arbitrage index was decreased based on the fact that the energy partner smart home bidding strategies reduced their profits.

As shown in Table 8, for the 2–4 cases, the expected average daily operational and energy not supplied costs, average daily locational marginal, and maximum and minimum values of daily locational marginal were increased when the percent of energy partner smart homes was increased. However, the average daily arbitrage index and the expected average number of switching to recover the system decreased when the energy partner smart homes percent was increased. For the fifth case, the A4-A7 and A9 variables were decreased when the energy partner smart homes percent was increased. Further, the average daily arbitrage index was increased based on the fact that the arbitrage opportunities for energy partners were increased.

It can be concluded that the increase of energy partner mode of smart homes may highly increase the operational costs of the system when these entities consider the arbitrage opportunities in their bidding strategies that may lead to reduce the resiliency of the system. Thus, the system operator should optimally dispatch the available energy resources of its system considering the arbitrage strategies of smart homes.

The simulation was carried out on a PC (AMD A10-5750M processor, 4*2.5 GHz, 8 GB RAM). The maximum simulation time for the normal operating condition of the 123-bus system was about 20,081 s. Further, the maximum simulation time for the worst-case contingent condition of the 123-bus system was about 732 s.

In conclusion, the proposed optimization algorithm successfully considered the arbitrage strategies of smart homes in the day-ahead and real-time horizons of distribution system scheduling for normal and contingent conditions. Further, the proposed model utilized the arbitrage index to explore the impacts of arbitrage of smart homes on the distribution system costs. Finally, the method considered the resiliency index in the optimization process for the day-ahead and real-time markets.

5. Conclusion

This paper introduced a multi-level multi-stage optimization process for optimal scheduling of distribution system resources in normal and contingent conditions of the system in the day-ahead and real-time horizons. The proposed algorithm considered the arbitrage and resiliency indices in the operational scheduling of the system and optimally dispatched the smart homes' energy resources to minimize the system costs and maximize the resiliency of the system. Further, the method sectionalized the distribution system into multi-microgrids to reduce the impacts of external shocks. The introduced algorithm was assessed for the 33-bus and 123-bus test systems and different external shock scenarios were considered. The proposed method reduced the expected values of aggregated system costs of 33-bus and 123-bus systems by about 62.14 % and 32.06 % concerning the cases that the smart homes performed arbitrage strategies.

CRediT authorship contribution statement

P. Jafarpour: Investigation, Data curation, Writing – original draft. M.S. Nazar: Conceptualization, Methodology, Supervision. M. Shafie-khah: Formal analysis, Validation. J.P.S. Catalão: Visualization, Writing – review & editing.

Declaration of competing interest

The authors declare that they have no known competing financial interests or personal relationships that could have appeared to influence the work reported in this paper.

Data availability

The data that has been used is confidential.

Acknowledgement

References

[1] Y. Yang, S. Wang, Resilient energy management with vehicle-to-home and photovoltaic uncertainty, Int. J. Electr. Power Energy Syst. 132 (2021), 107206.

[2] H. Afrakhte, P. Bayat, A contingency based energy management strategy for multi-microgrids considering battery energy storage systems and electric vehicles, J. Energy Storage 27 (2020), 101087.

[3] H. Mehrjerdi, Multilevel home energy management integrated with renewable energies and storage technologies considering contingency operation, J.Renew. Sustain.Energy 11 (2019), 025101.

[4] E. Rosales-Asensio, M. de Simón-Martín, D. Borge-Diez, J. Blanes-Peiró, A. Colmenar-Santos, Microgrids with energy storage systems as a means to increase power resilience: an application to office buildings, Energy 172 (2019) 1005–1015.

[5] R. Nourollahi, P. Salayani, K. Zare, B. Mohammadi Ivatloo, Resiliency-oriented optimal scheduling of microgrids the presence of demand response programs using a hybrid stochastic robust optimization approach, Int. J. Electr. Power Energy Syst. 128 (2021), 106723.

[6] G. Raman, J.C.H. Peng, T. Rahwan, Manipulating residents' behavior to attack the urban power distribution system, IEEE Trans.Ind.Inf. 15 (2019) 5575–5587.

[7] T. Sattarpour, D. Nazarpour, S. Golshannavaz, Load serving entity interactions on residential energy management strategy: a two-level approach, Sustain. Cities Soc. 40 (2018) 440–453.

[8] P. Srikantha, D. Kundur, Resilient distributed real-time demand response via population games, IEEE Trans.Smart Grid 8 (2016) 2532–2543.

[9] X. Liu, M. Shahidehpour, Z. Li, X. Liu, Y. Cao, Z. Bie, Microgrids for enhancing the power grid resilience in extreme conditions, IEEE Trans.Smart Grid 8 (2016) 589–597.

[10] M. Motalleb, M. Thornton, E. Reihani, R. Ghorbani, Providing frequency regulation reserve services using demand response scheduling, Energy Convers. Manag. 124 (2016) 439–452.

[11] K. Samarakoon, J. Ekanayake, N. Jenkins, Investigation of domestic load control to provide primary frequency response using smart meters, IEEE Trans.Smart Grid 3 (2011) 282–292.

[12] R. Yu, W. Yang, S. Rahardja, A statistical demand-price model with its application in optimal real-time price, IEEE Trans.Smart Grid 3 (2012) 1734–1742.

[13] A. Khodaei, Resiliency oriented microgrid optimal scheduling, IEEE Trans.Smart Grid 5 (2014) 1584–1591.

[14] B. Balasubramaniam, P. Saraf, R. Hadidi, E.B. Makram, Energy management system for enhanced resiliency of microgrids during islanded operation, Electr. Power Syst. Res. 137 (2016) 133–141.

[15] J.A. Short, D.G. Infield, L.L. Freris, Stabilization of grid frequency through dynamic demand control, IEEE Trans.Power Syst. 22 (2007) 1284–1293.

[16] M. Ali, A. Alahäivälä, F. Malik, M. Humayun, A. Safdarian, M. Lehtonen, A market-oriented hierarchical framework for residential demand response, Int. J. Electr. Power Energy Syst. 69 (2015) 257–263.

[17] A. Gholami, T. Shekari, F. Aminifar, M. Shahidehpour, Microgrid scheduling with uncertainty: the quest for resilience, IEEE Trans.Smart Grid 7 (2016) 2849–2858.

[18] K. Rahimi, M. Davoudi, Electric vehicles for improving resilience of distribution systems, Sustain. Cities Soc. 36 (2018) 246–256.

[19] N.Z. Xu, C.Y. Chung, Reliability evaluation of distribution systems including vehicle-to-home and vehicle-to-grid, IEEE Trans.Power Syst. 31 (2015) 759–768.

[20] H. Hosseinnia, J. Modarresi, D. Nazarpour, Optimal eco-emission scheduling of distribution network operator and distributed generator owner under employing demand response program, Energy 191 (2020), 116553.

[21] M.A. Fotouhi Ghazvini, J. Soares, O. Abrishambaf, R. Castro, Z. Vale, Demand response implementation in smart households, Energy Build. 143 (2017) 129–148.

[22] M. Rastegar, M. Fotuhi-Firuzabad, F. Aminifar, Load commitment in a smart home, Appl. Energy 96 (2012) 45–54.

[23] C. Gouveia, J. Moreira, C. Moreira, J.P. Lopes, Coordinating storage and demand response for microgrid emergency operation, IEEE Trans.Smart Grid 4 (2013) 1898–1908.

[24] H. Mehrjerdi, R. Hemmati, Coordination of vehicle-to-home and renewable capacity resources for energy management in resilience and self-healing building, Renew.Energy 146 (2020) 568–579.

[25] A. Eseye, M. Lehtonen, T. Tukia, S. Uimonen, R. Millar, Optimal energy trading for renewable energy integrated building microgrids containing electric vehicles and energy storage batteries, IEEE Access 7 (2019) 106092–106101.

[26] - F. Hafiz B. Chen C. Chen A.R. de Queiroz I. Husain "Utilising demand response for distribution service restoration to achieve grid resiliency against natural disasters", IET Gener. Transm. Distrib., 13, pp. 2942-2950.

[27] Z. Guo, G. Li, M. Zhou, W. Feng, Resilient configuration approach of integrated community energy system considering integrated demand response under uncertainty, IEEE Access 7 (2019) 87513–87533.

[28] Z. Wang, J. Wang, Self-healing resilient distribution systems based on sectionalization into microgrids, IEEE Trans.Power Syst. 30 (2015) 3139–3149.

[29] S.A. Arefifar, Y.A. Mohamed, T.H. El-Fouly, Comprehensive operational planning framework for self-healing control actions in smart distribution grids, IEEE Trans. Power Syst. 28 (2013) 4192–4200.

[30] H. Farzin, M. Fotuhi-Firuzabad, M. Moeini-Aghtaie, Enhancing power system resilience through hierarchical outage management in multi-microgrids, IEEE Trans.Smart Grid 7 (2016) 2869–2879.

[31] A. Hussain, V.H. Bui, H.M. Kim, Resilience-oriented optimal operation of networked hybrid microgrids, IEEE Trans.Smart Grid 10 (2017) 204–215.

[32] A. Hussain, V.H. Bui, H.M. Kim, A resilient and privacy-preserving energy management strategy for networked microgrids, IEEE Trans.Smart Grid 9 (2016) 2127–2139.

[33] T. Khalili, M. Tarafdar Hagh, S. Gassem Zadeh, S. Maleki, Optimal reliable and resilient construction of dynamic self-adequate multi-microgrids under large-scale events, IET Gener. Transm. Distrib. 10 (2019) 1750–1760.

[34] S. Chanda, A.K. Srivastava, Defining and enabling resiliency of electric distribution systems with multiple microgrids, IEEE Trans.Smart Grid 7 (2016) 2859–2868.

[35] J. Zhu, Y. Yuan, W. Wang, An exact microgrid formation model for load restoration in resilient distribution system, Int. J. Electr. Power Energy Syst. 116 (2020), 105568.

[36] A. Hussain, V.H. Bui, H.M. Kim, Microgrids as a resilience resource and strategies used by microgrids for enhancing resilience, Appl. Energy 240 (2019) 56–72.

[37] H. Zakernezhad, M. Setayesh Nazar, M. Shafie-khah, J.P.S. Catalão, Optimal scheduling of an active distribution system considering distributed energy resources, demand response aggregators and electrical energy storage, Appl. Energy 314 (2022), 118865.

[38] S.Najafi Ravadanegh, S. Jamali, A.Mohammadi Vaniar, Multi-infrastructure energy systems resiliency assessment in the presence of multi-hazards disasters, Sustain. Cities Soc. 79 (2022), 103687.

[39] C. Lin, C. Chen, F. Liu, G. Li, Z. Bie, Dynamic MGs-based load restoration for resilient urban power distribution systems considering intermittent RESs and droop control, Int. J. Electr. Power Energy Syst. 140 (2020), 107975.

[40] M. Diahovchenko, G. Kandaperumal, A.K. Srivastava, Z.I. Maslova, S.M. Lebedka, Resiliency-driven strategies for power distribution system development, Electr. Power Syst. Res. 197 (2021), 107327.

[41] M. Alilou, B. Tousi, H. Shayeghi, Home energy management in a residential smart micro grid under stochastic penetration of solar panels and electric vehicles, Sol. Energy 212 (2020) 6–18.

[42] - H. Nezamabadi M. Setayesh Nazar , "Arbitrage strategy of virtual power plants in energy, spinning reserve and reactive power markets", IET Gener. Transm. Distrib., 10, pp. 750-763.

[43] A. Eichhorn, H. Heitsch, W. Römisch, Stochastic optimization of electricity portfolios: scenario tree modeling and risk management, in: Handbook of Power Systems II, Springer, Berlin, Heidelberg, 2010.

[44] H. Heitsch, W. Römisch, Scenario reduction algorithms in stochastic programming, Comput.Optim.Applic. 24 (2003) 187–206.

[45] A. Bostan, M. Setayesh Nazar, M.R. Shafie-khah, J.P.S. Catalão, An integrated optimization framework for combined heat and power units, distributed generation and plug-in electric vehicles, Energy 202 (2020) 117789.

[46] A. Bostan, M. Setayesh Nazar, M.R. Shafie-khah, J.P.S. Catalão, Optimal scheduling of distribution systems considering multiple downward energy hubs and demand response programs, Energy 190 (2020), 116349.